

Time-(ir)reversibility in active matter: from micro to macro

J. O’Byrne¹, Y. Kafri², J. Tailleur¹, F. van Wijland¹

¹*Université de Paris, MSC, UMR 7057 CNRS, 75205 Paris, France*

²*Department of Physics, Technion, Haifa, 32000, Israel*

Active matter encompasses systems whose individual constituents dissipate energy to exert propelling forces on their environment. This rapidly developing field harbors a dynamical phenomenology with no counterpart in passive systems. The extent to which this is rooted in the breaking of time-reversibility has recently triggered an important theoretical and experimental activity which is the focus of this review. Building on recent progress in the field, we disentangle the respective roles of the arrow of time and of the non-Boltzmann nature of steady-state fluctuations in single- and many-body active systems. We show that effective time-reversible descriptions of active systems may be found at all scales, and discuss how interactions, either between constituents or with external operators, may reveal the non-equilibrium nature of the microscopic source of energy. At a time when the engineering of active materials appears within our reach, this allows us to discuss to which extent methods stemming from equilibrium statistical mechanics may guide us in their design.

1 Introduction

Active matter describes systems whose fundamental constituents dissipate energy to exert self-propelling forces on the environment. From birds to bacteria, from cells to molecular motors, the biological world is filled with active entities. Indeed, active matter was initially strongly driven by its biophysical applications (Fig 1a-b). Since then, a wealth of synthetic active systems have been engineered in the lab, which now pave the way towards the engineering of synthetic active materials (Fig 1c-e). However, many fundamental questions need to be addressed before one may reach the level of complexity relevant for material design or to decipher the physical laws involved in biological processes, from morphogenesis to the large-scale organization of complex ecosystems.

In addition to its potential implications for biophysics and material design, the upsurge of interest in active matter also stems from its rich dynamical phenomenology, which is largely without counterpart in passive systems and has been extensively reviewed previously^{18,38,40,80,126,161,202}. This emerging physics stems from a microscopic nonequilibrium drive at the particle level that

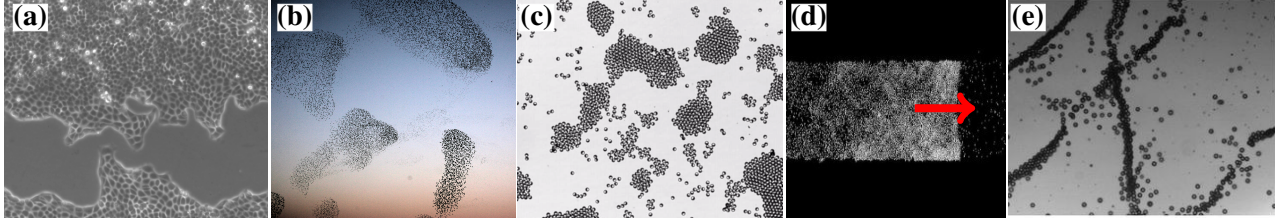


Figure 1: Active matter systems are commonly found in nature (a-b) and engineered in the lab (c-e). **(a)** Monolayer of cells invading an artificial wound ¹⁵⁰ (Copyright (2007) National Academy of Sciences). **(b)** Bird flocks undergoing collective motion ²² (Credits COBBS Lab, Institute for Complex Systems, Rome). **(c)** Interrupted motility-induced phase separation in self-propelled colloids ¹⁹⁷ (Courtesy of O. Dauchot). **(d)** Non-linear travelling wave of Quincke colloidal rollers ³¹ (Courtesy of D. Bartolo and A. Morin). **(e)** Dynamic lane formation and breaking by self-propelled droplets ¹⁹².

leads to system-dependent violations of two hallmark features of thermal equilibrium: time-reversal symmetry (TRS) and Boltzmann statistics. For instance, the lack of TRS, when accompanied by the spontaneous emergence of macroscopic currents, is at the root of flocking behaviours, whether observed in groups of animals (Fig. 1b) or engineered in synthetic self-propelled colloids (Fig. 1d). Nothing prevents, however, the orientations of the birds within a flock to display an equilibrium-like statistics ¹³². Conversely, the emergence of self-assembled clusters in the absence of attractive forces shown in Fig. 1c transcends the constraints imposed by the Boltzmann weight. No manifest arrow of time is, however, observed in the corresponding motility-induced phase separation. The aim of this review is to disentangle the respective roles of the violations of TRS and of Boltzmann statistics in active matter and to discuss the vast literature which touches on these questions. At a time when the design of active materials has become a practical challenge, the existence of an effective TRS—and of its accompanying equilibrium toolbox— has become a central question.

This review is intended both for newcomers in the field of active matter as well as for condensed-matter and biophysics specialists. As such, it relies on general concepts of statistical mechanics and stochastic processes. We start by discussing the Langevin description of active particles in section 2, which we contrast with the Brownian dynamics of colloidal particles. We explain the meaning of TRS in this stochastic context and how TRS violations can be measured using the entropy production rate introduced in stochastic thermodynamics. We discuss the ambiguities that naturally emerge when characterizing the TRS of coarse-grained systems, which we loosely understand as integrating out some of the degrees of freedom. We illustrate this discussion

by considering a free active particle whose position and orientation are recorded over time. TRS violation is demonstrated by a non-vanishing entropy production rate equal to the energy dissipated by the active force powering the motion. Measuring solely the particle position, however, restores TRS and leads to a vanishing entropy production rate.

We then turn in section 3 to the case of non-interacting active particles subjected to external potentials. We discuss how non-Boltzmann features emerge in this context. In particular, we compare the non-local dependency of the steady-state distribution on the external potential for different types of active particles. In addition, external potentials also lead to TRS violations, under the form of non-vanishing entropy production rates and steady-state currents. Conversely, we discuss the conditions under which an effective thermal equilibrium regime is recovered or a TRS is restored.

Finally, section 4 discusses the case of interacting active particles. We focus in particular on Motility-Induced Phase Separation (MIPS) whose macroscopic dynamics resembles an equilibrium phase separation despite a microscopic nonequilibrium drive at the particle level, which makes it interesting from a TRS perspective. We show how TRS violations can nevertheless be identified using field-theoretical methods and how they impact the construction of the phase diagram. We also discuss cases in which TRS is exactly restored at the macroscopic scale, either by considering specific classes of active systems endowed with tactic interactions or in the small-persistence-time limit.

2 TRS of a single active-particle: in and out of equilibrium

Sources and sinks of energy in active matter. Let us consider the simplest model of an active particle

$$m\ddot{\mathbf{r}} = -\gamma\dot{\mathbf{r}} + \mathbf{f}_p(t) - \nabla V(\mathbf{r}) + \sqrt{2\gamma^2 D}\boldsymbol{\eta}(t) \quad (1)$$

Here, \mathbf{r} is the position of the particle, $-\gamma\dot{\mathbf{r}}$ a viscous damping term, \mathbf{f}_p the self-propulsion force, $V(\mathbf{r})$ an external potential, and $\boldsymbol{\eta}$ a Gaussian white noise that may represent thermal noise or other fluctuation sources. The self-propulsion force \mathbf{f}_p is a defining feature of active matter: it is a time-dependent, non-conservative force, endowed with a particle-dependent stochastic dynamics, and powered by an irreversible consumption of energy. The presence of self-propulsion forces both drive active systems out of thermal equilibrium and distinguish active matter from other nonequilibrium systems, such as glasses or boundary driven fluids whose bulk dynamics is of equilibrium nature. The energy source powering \mathbf{f}_p varies from system to system: it can be a local field, as in

Janus self-phoretic colloids^{90,142,143} or bacteria^{19,38}, or it can stem from a global external field, as for vibrated grains⁵², Quincke rollers³¹, or bi-electric colloids under AC fields^{139,197,213}. The dynamics of \mathbf{f}_p can be equally diverse and can, for instance, include rotational diffusion or tumbles of its orientation, as well as fluctuations in its amplitude.

A natural question is whether one could subsume $\mathbf{f}_p(t)$ and $\sqrt{2\gamma^2 D}\boldsymbol{\eta}(t)$ into a single noise source $\tilde{\boldsymbol{\eta}}(t)$ and treat Eq. (1) as an effective equilibrium Langevin dynamics. The answer comes from thermodynamics: the main difference between passive and active particles lies in the injection of energy. For passive particles, the fluid is responsible both for the dissipation and the injection of energy (Fig. 2, left). The former results from the average force exerted by the fluid on the particle, $-\gamma\dot{\mathbf{r}}$, with a corresponding dissipated power $-\gamma\dot{\mathbf{r}}^2$. On the contrary, the latter stems from fluctuations of the fluid forces around their mean, $\sqrt{2\gamma^2 D}\boldsymbol{\eta}(t)$, which inject a mean power $d\gamma^2 D/m$. When the fluid is at equilibrium, injection and dissipation of energy are related by the celebrated fluctuation-dissipation theorem through $D = kT/\gamma$. For an active particle, on the contrary, most of the injection of energy comes from the self-propulsion force and it is thus physically disconnected from dissipation: $\tilde{\boldsymbol{\eta}}(t)$ would not satisfy a fluctuation-dissipation relation (See Fig. 2, right). Note that this discussion assumes that \mathbf{f}_p is not a Gaussian white noise, otherwise it could indeed be absorbed in $\boldsymbol{\eta}(t)$ at the cost of a simple quantitative shift of the temperature. This observation is the motivation for most models of active particles considered in the literature that rely on variations of Eq. (1) with noises and drags not related by (generalized) Stokes-Einstein relations.

Since most active systems live at low Reynolds numbers, the overdamped limit of the Langevin dynamics is often assumed, although the role of inertia has recently attracted interest^{10,48,51,111,123,125}. Three standard models of active particles are described by the dynamical equation

$$\dot{\mathbf{r}} = \mathbf{v}_p - \mu\nabla V(\mathbf{r}) + \sqrt{2D}\boldsymbol{\eta}(t) \quad (2)$$

where $\mu = \gamma^{-1}$ is the particle mobility and $\mathbf{v}_p = \mu\mathbf{f}_p$ its self-propulsion velocity. For Active Brownian particles (ABPs) and Run-and-Tumble particles (RTPs), the magnitude of \mathbf{v}_p is constant, while its orientation undergoes either rotational diffusion or random, Poisson-distributed reorientation events. On the contrary, an Active Ornstein-Uhlenbeck particle (AOUP) has a self-propulsion velocity whose modulus fluctuates and is given by an Ornstein-Uhlenbeck process $\dot{\mathbf{v}}_p = -\mathbf{v}_p/\tau + \sqrt{2D\tau^2}\boldsymbol{\xi}$, with $\boldsymbol{\xi}$ a Gaussian white noise with unit amplitude. Using angular brackets to denote averages over the dynamics of the self-propulsion velocities, the temporal correlation of $\langle \mathbf{v}_p(t)\mathbf{v}_p(0) \rangle$ can be equal in the three models. The physics of their self-propulsion, however, is quite different: the probability distribution of \mathbf{v}_p is Gaussian and peaked around $\mathbf{0}$ for

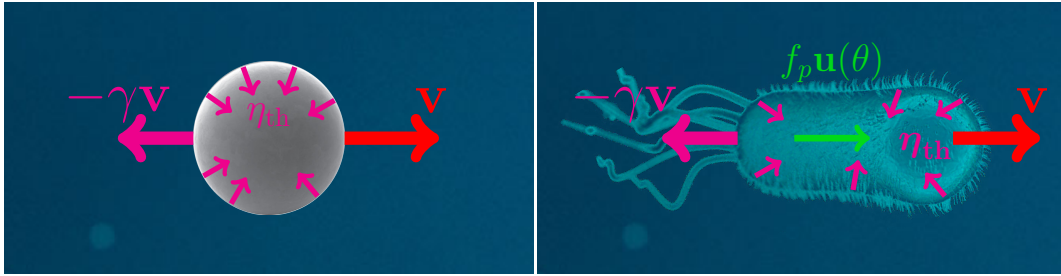


Figure 2: Colloidal dynamics resulting from interactions with fluid molecules (**left**). The mean resulting force is a drag $-\gamma\mathbf{v}$, which dissipates energy by opposing motion, whereas fluctuations around it, described by the Gaussian white noise η_{th} , inject energy into the colloid's dynamics. When the fluid is in equilibrium, injection and dissipation are related by the fluctuation-dissipation theorem. On the contrary, the propulsion of a bacterium (**right**), stems from the consumption of a separate energy source, which is disconnected from the dissipation. In the steady state, the energy balance between sources and sinks of energy is given by $\langle \mathbf{f}_p \cdot \dot{\mathbf{r}} \rangle + \frac{d\gamma^2 D}{m} = \gamma \langle \dot{\mathbf{r}}^2 \rangle$, which can be derived from Eq. (1) in d space dimensions by computing the time derivative of $m\dot{\mathbf{r}}^2/2$. The dissipation $w_p = \langle \mathbf{f}_p \cdot \dot{\mathbf{r}} \rangle$ measures the energy per unit time injected by the self-propulsion force into the system; it violates the equipartition $\frac{1}{2}m\langle \dot{\mathbf{r}}^2 \rangle = \frac{1}{2}d\gamma D$ that would otherwise be satisfied for an equilibrated colloid. It is the microscopic signature of activity.

AOUPs, whereas it is uniform on a sphere of fixed radius for ABPs and RTPs.

Note that the discussion above for the translational degree of freedom \mathbf{r} can be extended to rotational ones. In particular, this leads to a class of particles called spinors, in which self-propulsion speed is replaced with a self torque or, more generally, the rotational noise and damping do not satisfy a Stokes-Einstein relation. These systems have been studied both at the theoretical^{6,81,107,137,200,216} and experimental^{32,97,162,178} levels.

An immediate consequence of the absence of the Stokes-Einstein relation is that, in the presence of an external potential V , the stochastic dynamics of an active particle does not necessarily lead to a steady state given by a Boltzmann weight $P_{\text{eq}}(\mathbf{r}) \propto \exp[-\beta V(\mathbf{r})]$. This leads to a host of interesting phenomena that we partly review in Section 3. Note, however, that while the Boltzmann weight may be the textbook definition of equilibrium statistical mechanics, a broader definition of equilibrium is based on dynamics; it equates with TRS in the steady state, under the form of a detailed-balance relation. We now discuss the origin of the latter and its rather subtle fate for active particles.

Equilibrium & time-reversal symmetry. The dynamics of a system is said to be time-reversal symmetric if observing a trajectory or its time-reversal are equally likely: $P[\{\mathbf{r}(\tau), 0 \leq \tau \leq t\}] = P[\{\mathbf{r}(t - \tau), 0 \leq \tau \leq t\}]$, which, using the definition of conditional probability, can equally be written as

$$P[\{\mathbf{r}(\tau), 0 < \tau \leq t\}|\mathbf{r}(0)]P_s(\mathbf{r}(0)) = P[\{\mathbf{r}(t - \tau), 0 < \tau \leq t\}|\mathbf{r}(t)]P_s(\mathbf{r}(t)) . \quad (3)$$

Here $P_s(\mathbf{r})$ is the (stationary) probability to sample a configuration \mathbf{r} whereas $P[\{\mathbf{r}(\tau), 0 \leq \tau \leq t\}|\mathbf{r}(0)]$ is the probability of any trajectory $\{\mathbf{r}(\tau)\}$ starting from $\mathbf{r}(0)$. In the following, we restrict ourselves to Markovian dynamics for simplicity, even though the discussion can be generalized to non-Markovian processes. $P[\{\mathbf{r}(\tau), 0 < \tau \leq t\}|\mathbf{r}(0)]$ is then the average probability that a trajectory passing through $\mathbf{r}(0)$ at 0 will follow $\{\mathbf{r}(\tau)\}$. Microscopically, Eq. (3) is granted by the laws of classical mechanics and directly applies if \mathbf{r} describes both a colloidal particle and the surrounding fluid molecules. Mesoscopically, however, when \mathbf{r} solely describes the colloidal particle, Eq. (3) requires a statistical hypothesis on the distribution of the fluid degrees of freedom which have been coarse-grained out (See Box *Microscopic vs statistical reversibility*). In equilibrium, this is given by Boltzmann microcanonical hypothesis. For more general systems, coarse-graining out the fluid degrees of freedom need not lead to dynamics obeying a statistical time-reversal symmetry. A whole set of theoretical tools have thus been developed to test whether stochastic dynamics such as Eq. (1) or (2) satisfy TRS or not (See Box *Identifying time-reversal symmetry breaking*).

Microscopic vs statistical reversibility. Consider a colloidal particle embedded in an equilibrated fluid. When considering the full system, {Fluid + Colloid}, time-reversibility is given by Eq. (3), where $\mathbf{r}(s)$ describes the joint degrees of freedom of the colloid and of the fluid molecules. The time-reversibility of Hamilton's equations of motion ensures that $P[\{\mathbf{r}(\tau), 0 \leq \tau \leq t\}|\mathbf{r}(0)] = P[\{\mathbf{r}(t - \tau), 0 \leq \tau \leq t\}|\mathbf{r}(t)]$. This directly leads to $P_s(\mathbf{r}(0)) = P_s(\mathbf{r}(t))$: the probability is conserved along the trajectory, as guaranteed by Liouville theorem.

If $\mathbf{r}(s)$ now refers to the colloid only, then $P[\{\mathbf{r}(\tau), 0 \leq \tau \leq t\}|\mathbf{r}(0)]$ is given by the measure of all initial conditions of the fluid molecules which are compatible with the trajectory of the colloid. Assuming microcanonical equilibrium, a scale separation between the fluid molecules and the colloid, and denoting by $E(\mathbf{r})$ and E_{tot} the energies of the colloid and of the total system, the measure of these initial conditions is given by $\Omega_{\text{traj}}/\Omega_{\text{fl}}[E_{\text{tot}} - E(\mathbf{r}(0))]$. Here, $\Omega_{\text{fl}}[E_{\text{tot}} - E(\mathbf{r}(0))]$ is the phase-space volume of all fluid configurations at energy $E_{\text{tot}} - E(\mathbf{r}(0))$ and Ω_{traj} is that of the initial conditions compatible with the colloid trajectory. Conversely, the probability of the time-reversed trajectory is given by $\Omega_{\text{traj}}/\Omega_{\text{fl}}[E_{\text{tot}} - E(\mathbf{r}(t))]$, which now differs from that of the forward trajectories if the energy of the colloid has changed. The time-reversal condition (3) then simplifies into

$$P_s(\mathbf{r}(0)) \exp[E(\mathbf{r}(0))/kT] = P_s(\mathbf{r}(t)) \exp[E(\mathbf{r}(t))/kT] \quad (4)$$

where we have used that $\Omega_{\text{fl}}(E_{\text{tot}} - E(\mathbf{r})) \propto \exp(-E(\mathbf{r})/kT)$ with T the temperature of the fluid, defined as $T^{-1} = k \frac{\partial \log \Omega_{\text{fl}}}{\partial E} \Big|_{E_{\text{tot}}}$. Equation (4) enforces the Boltzmann weight as a steady-state distribution for the colloidal particle.

Unlike the microscopic reversibility of Hamilton's equations of motion, the statistical reversibility of the colloid's dynamics requires a statistical hypothesis for the fluid molecules, which is here given by the microcanonical postulate. Another distribution for the fluid molecules would typically have led to a violation of Eq. (3): statistical irreversibility for the colloidal dynamics thus generically emerges from a microscopically reversible dynamics once the bath's degrees of freedom have been coarse-grained out.

Identifying time-reversal symmetry breaking. The question of TRS and its breakdown arises in many different settings and formalisms, whether using Langevin dynamics or jump processes, for underdamped or overdamped dynamics, at the level of particles or fields. Its identification relies on an equally diverse set of tools^{74,199}, which we illustrate for the simple setting of an

overdamped Brownian dynamics in the presence of a force field $\mathbf{F}(\mathbf{r})$:

$$\dot{\mathbf{r}} = \mu\mathbf{F}(\mathbf{r}) + \sqrt{2D}\boldsymbol{\eta}, \quad (5)$$

where $\boldsymbol{\eta}$ is a unit Gaussian white noise and D and μ positive constants. For such Markovian dynamics, the TRS defined in Eq. (3) can be read at several levels.

- TRS amounts to an equality in the steady state of the joint two-time probability density $p(\mathbf{r}_1, t; \mathbf{r}_2, 0) = p(\mathbf{r}_2, t; \mathbf{r}_1, 0)$. This generalizes to any pairs of observables $A(\mathbf{r})$ and $B(\mathbf{r})$ where TRS implies $C_{AB}(t) = C_{BA}(t)$ with $C_{AB}(t) = \langle A(t)B(0) \rangle$. In experiments or simulations, measuring a non-vanishing $\Delta_{AB}(t) \equiv [C_{AB}(t) - C_{BA}(t)]/2$ offers a low-dimensional *sufficient* condition to prove a violation of TRS. $\Delta_{AB}(t)$ is the time anti-symmetric part of the correlation function $C_{AB}(t)$, an idea which can be generalized to other observables¹¹⁵.
- The probability density $P(\mathbf{r}, t)$ evolves according to a Fokker-Planck equation $\partial_t P = -HP$. TRS is equivalent to a symmetry of the Fokker-Planck operator: $H^\dagger = P_S^{-1}HP_S$, where P_S is the stationary measure and H^\dagger is the adjoint of H (for the L^2 scalar product). In particular, this implies the existence of a basis in which H becomes Hermitian and that it has a real spectrum¹⁵⁷. For overdamped Brownian dynamics with additive noise, this has been used to endow H with a supersymmetric structure akin to that of Schrödinger's equation^{190,206}.
- The Fokker-Planck equation can be read as a conservation equation for a probability current $\mathbf{J}(\mathbf{r}) = \mu\mathbf{F}(\mathbf{r})P(\mathbf{r}) - D\nabla P(\mathbf{r})$. TRS is equivalent to the vanishing of \mathbf{J} in the steady state. The experimental measurement of such a high dimensional object is difficult, but its projection on a finite set of relevant degrees of freedom has recently been used to sample TRS breakdown in biological systems^{16,78,79}.
- Another measure of TRS breakdown is obtained by computing:

$$\Sigma(0, t_f) = \int D[\{\mathbf{r}(t)\}] P[\{\mathbf{r}(t)\}] \hat{\Sigma}[\{\mathbf{r}(t)\}] = \int D[\{\mathbf{r}(t)\}] P[\{\mathbf{r}(t)\}] \log \frac{P[\{\mathbf{r}(t)\}]}{P[\{\mathbf{r}(t_f - t)\}]}.$$

Mathematically, Σ is the Kullback-Leibler divergence between the probabilities of backward and forward paths and $\hat{\Sigma}$ can be seen as a 'path-wise entropy production'¹⁶⁷. For dynamics (5), Σ can be decomposed between the heat transferred to the thermal bath and the variation of the Gibbs-Shannon entropy of the measure $P(\mathbf{r}, t)$ ^{87,167}. The positivity of Σ generalizes the second law of Thermodynamics to microscopic systems described by Langevin equations. In turn, the entropy production rate, defined as:

$$\sigma \equiv \lim_{t_f \rightarrow \infty} \frac{1}{t_f} \Sigma(0, t_f), \quad (6)$$

is a direct measurement of the irreversibility of the dynamics^{101,103,113} that is commonly used in non-equilibrium statistical mechanics, even in the absence of any connection to Thermodynamics^{46,116}.

Of course, the four criteria discussed above are not independent from each other. For instance, for dynamics (5), the steady-state entropy production rate is connected to the probability current $\mathbf{J}(\mathbf{r})$ defined above through:

$$\sigma = \frac{\mu}{D} \int d\mathbf{r} \frac{\mathbf{J}^2(\mathbf{r})}{P_s(\mathbf{r})}.$$

From the knowledge of the dynamics, conditions can be derived for TRS to be violated. For dynamics (5), irreversibility requires the existence of a closed loop \mathcal{C} such that:

$$\oint_{\mathcal{C}} \mathbf{F}(\mathbf{r}) \cdot d\mathbf{r} \neq 0$$

This criterion generalizes the Kolmogorov criterion derived for Markov chains¹⁹⁹. Mathematically, \mathbf{F} needs to contain a curl or a harmonic part⁹¹. Conversely, TRS imposes a direct relation between the force field \mathbf{F} and the steady-state probability: $\mu\mathbf{F} = D\nabla \log P_s$. All the discussion above generalizes—under more complex forms—to other dynamics, for instance involving variables which are odds under time-reversal symmetry^{74,199}.

TRS in active matter. For equilibrium systems, TRS is ensured irrespectively of the degree of coarse graining and holds both for microscopic and coarse-grained mesoscopic descriptions. For active systems, on the contrary, this question is more subtle and the possible existence of TRS depends on the degrees of freedom which are being considered. This makes its characterization—in particular using an entropy production rate defined in the spirit of Eq. (6)—a somewhat ambiguous task, which has attracted a lot of interest both theoretically^{29,36,46,47,68,73,84,124,128,134,160,169,184} and experimentally^{16,65,66,78,79,131,159,205}.

To illustrate this, consider a zero-Reynolds swimmer at position $\mathbf{r}(t)$ moving through a fluid thanks to the displacement of some degrees of freedom $\mathbf{x}_i(t)$. (Think about the motion of a flagellum.) The solution of Stokes equation will lead to a flow $\mathbf{u}(t)$ and a self-propulsion speed $\mathbf{v}_p(t)$, which results from a propulsion force $\mathbf{f}(t)$ exerted on the fluid. (By Newton third law, \mathbf{f} is equal and opposite to \mathbf{f}_p in Eq. (1).) A recording of $\mathbf{r}(t)$ and $\mathbf{x}_i(t)$ of duration t_f played backward is also a solution of Stokes equation. It would involve a force $-\mathbf{f}(t_f - t)$, a speed $-\mathbf{v}_p(t_f - t)$ and a flow $-\mathbf{u}(t_f - t)$. It is, however, distinguishable from the forward trajectory: our swimmer will swim

backward, a ‘pusher’ would become a ‘puller’. In probabilistic terms, the trajectory $\mathbf{r}(t)$ given the displacements $\mathbf{x}_i(t)$ is equally likely to occur as $\mathbf{r}(t_f - t)$ given $\mathbf{x}_i(t_f - t)$, even though they can be distinguished by the flow they generate.

The situation is reminiscent of the equilibrium Langevin dynamics of a passive charged particle at $\mathbf{r}(t)$ in a magnetic field $\mathbf{B}(t)$ created by electrons at positions $\mathbf{x}_i(t)$, moving deterministically in a coil:

$$m\ddot{\mathbf{r}} = -\gamma\dot{\mathbf{r}} + q\dot{\mathbf{r}} \times \mathbf{B}(t) + \sqrt{2\gamma kT}\boldsymbol{\eta}, \quad (7)$$

with q the charge of the particle, γ its damping coefficient, m its mass, and kT the temperature. The reverse trajectories $\mathbf{x}_i(t_f - t)$ lead to a magnetic field $-\mathbf{B}(t_f - t)$ so that $\mathbf{r}(t_f - t)$ is equally likely to occur as $\mathbf{r}(t)$ was in the presence of $\mathbf{B}(t)$. Mathematically, the conditional probabilities of observing $\mathbf{r}(t)$ given $\mathbf{x}_i(t)$ and $\mathbf{r}(t_f - t)$ given $\mathbf{x}_i(t_f - t)$ are thus equal and the corresponding entropy production rate vanishes $\sigma = \lim_{t \rightarrow \infty} \frac{1}{t} \log \frac{P[\{\mathbf{r}(t)\}|\{\mathbf{x}_i(t)\}]}{P[\{\mathbf{r}(t_f - t)\}|\{\mathbf{x}_i(t_f - t)\}]} = 0$, consistently with thermodynamics. In a given experiment, however, it is not the conditional probability which is measured, but the joint probability of observing $\mathbf{r}(t)$ and $\mathbf{x}_i(t)$. When the electrons are driven by a fixed potential difference, for instance, they will not generate $\mathbf{x}_i(t)$ and $\mathbf{x}_i(t_f - t)$ with equal probability. The observation of $\mathbf{r}(t)$ and $\mathbf{r}(t_f - t)$ will thus not be equally likely: they do not inherit the underlying TRS dynamics (7) would have if the dynamics of $\mathbf{x}_i(t)$ were time reversible. This ‘induced’ irreversibility can be measured by comparing the occurrence frequency of $\mathbf{r}(t)$ and $\mathbf{r}(t_f - t)$ for the same field $\mathbf{B}(t) = \mathbf{B}_0$. The corresponding ‘Shannon’ entropy production rate is now finite, given by $\sigma = 2q^2|\mathbf{B}_0|^2/(\gamma m)$. Note that this ‘entropy-production rate’ solely measures the irreversibility of the trajectories $\mathbf{r}(t)$ in an experiment with a fixed magnetic field. In particular, it is not a measure of the creation of thermodynamic entropy in our magnetic system since the magnetic field has to be flipped under time-reversal. Equation (7) has also been used to describe the hair bundle of sensory cells⁵⁶. There, the term analogous to $\mathbf{B}(t)$ has a different origin and does not flip under time reversal and thus leads to a non-vanishing thermodynamic entropy production rate. Whether a given definition of σ can be connected to the thermodynamic entropy production rate or not depends on the physics of the system under study; it can always be connected to a measure of irreversibility in the sense described above, which is the perspective adopted in this review.

In active matter, the internal processes leading to $\mathbf{x}_i(t)$ are often strongly irreversible. In living systems, they rely on an imbalance between the concentrations of ATP and ADP+P^{3,92} in the cells. For Janus self-diffusiophoretic colloids, it is the irreversible transmutation of hydrogen peroxide into oxygen and water^{90,142} which powers self-propulsion. The observation of

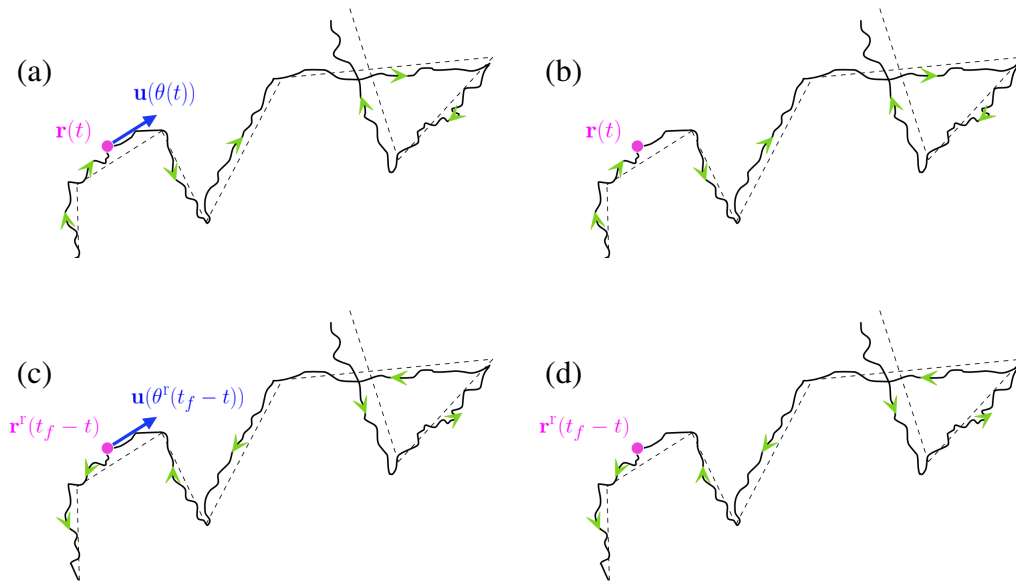


Figure 3: Trajectories of a run-and-tumble particle experiencing translational noise. The noise-less trajectory is drawn as a dashed line and the direction of time is indicated by green arrows. One may record the position and orientation of the particle (a) or solely its position (b). The time-reversed trajectories of (a) and (b) are shown in (c) and (d). Their likeliness are clearly different since the noise has to fight self-propulsion in (c), but not necessarily in (d).

$\mathbf{r}(t)$ and $\mathbf{r}(t_f - t)$ thus need not occur with equal probabilities. (An interesting exception is when self-propulsion emerges from spontaneous symmetry breaking as in Quincke rollers³¹.) It is this induced irreversibility that will be discussed in the rest of this article. Before turning to the corresponding computation of the entropy production rate, let us stress that the most irreversible process in active system is, generically, the one generating $\mathbf{x}_i(t)$, and not the dynamics of $\mathbf{r}(t)$. When trying to measure the energy dissipated in an active system, say using calorimetry, one would expect that this process strongly dominates all other sources of irreversibility. A large part of the irreversibility is thus lost if the irreversible process leading to the active force is not modelled^{47,147}. This is, in particular, the case of Eq. (1) in which the active force is an input of the problem whose origin is unspecified. The ‘dissipation’ measured through $w_p = \langle \mathbf{f}_p \cdot \dot{\mathbf{r}} \rangle$ thus cannot capture the full irreversibility of the system. As we show below, it is nevertheless an interesting object of study since it quantifies the violation of TRS encapsulated in the degrees of freedom $\mathbf{r}(t)$ and $\mathbf{f}_p(t)$.

Let us first show that, even at the level of dynamics (1), the existence of TRS remains ambiguous and depends on which degrees of freedom are under study. We start by considering the situation depicted in Fig. 3, which compares the trajectory of a model run-and-tumble bacteria in two space dimensions with its time-reversed counterpart. The underlying stochastic dynamics is given by

$$\dot{\mathbf{r}}(t) = v_0 \mathbf{u}(\theta(t)) + \sqrt{2D} \boldsymbol{\eta}(t) \quad (8)$$

where v_0 is a fixed self-propulsion speed and $\theta(t)$ is fully randomized at rate α . The trajectory presented in Fig. 3a records the time evolution of both the particle position $\mathbf{r}(t)$ and its orientation $\theta(t)$. Note that $\mathbf{r}(t)$ and $\theta(t)$ uniquely characterize the realization of the noise through $\sqrt{2D} \boldsymbol{\eta}(t) = \dot{\mathbf{r}}(t) - v_0 \mathbf{u}(\theta(t))$. As detailed in Appendix A, for the reversed trajectory $\mathbf{r}^r(t) = \mathbf{r}(t_f - t)$, $\theta^r(t) = \theta(t_f - t)$ to be observed, the surrounding fluid molecules have to produce a different noise $\boldsymbol{\eta}^r(t)$ such that $\sqrt{2D} \boldsymbol{\eta}^r(t) = -\sqrt{2D} \boldsymbol{\eta}(t_f - t) - 2v_0 \mathbf{u}(\theta(t_f - t))$. This shows that time-reversed trajectories are obtained by making the noise $\boldsymbol{\eta}^r$ work against the active force to make the active particle retrace its steps. Using the Gaussian weights of these two noise realizations, their relative probability to occur can be computed, leading to a path-wise entropy production (See Box *Identifying time-reversal symmetry breaking*):

$$\hat{\Sigma}[\{\mathbf{r}(t), \theta(t)\}] = \frac{\mu}{D} \int_0^{t_f} dt \dot{\mathbf{r}} \cdot \mathbf{f}_p + \log \frac{P_0(\mathbf{r}_0, \theta_0)}{P_f(\mathbf{r}_f, \theta_f)}, \quad (9)$$

where $P_f(\mathbf{r}_f, \theta_f)$ is the probability of being at $\mathbf{r}_f \equiv \mathbf{r}(t_f)$ and $\theta_f \equiv \theta(t_f)$ given that the initial condition was sampled according to P_0 . The right-hand side of Eq. (9) measures both the heat transferred to the bath, $-\hat{Q} \equiv \int_0^{t_f} \dot{\mathbf{r}} \cdot \mathbf{f}_p dt$, and the change in the ‘stochastic’ Shannon entropy $\Delta \hat{S} = \log \frac{P_0(\mathbf{r}_0, \theta_0)}{P_f(\mathbf{r}_f, \theta_f)}$ between P_0 and P_f associated to the trajectory $\{\mathbf{r}(t), \theta(t)\}$ ¹⁶⁷. Taking the average over the forward path probability, and using the positivity of the Kullback-Leibler divergence, leads to a generalized second law $\langle \Delta \hat{S} \rangle > \frac{\mu}{D} \langle \hat{Q} \rangle$. Alternatively, taking the limit $t_f \rightarrow \infty$, leads to the steady-state entropy production *rate*

$$\sigma = \lim_{t_f \rightarrow \infty} \frac{1}{t_f} \hat{\Sigma} = \frac{\mu \langle \dot{\mathbf{r}} \cdot \mathbf{f}_p \rangle}{D} = \frac{\mu w_p}{D}, \quad (10)$$

where we have used the ergodicity of the dynamics. The average dissipation of the active force w_p thus measures the irreversibility of the active dynamics (8)^{34,136}. The latter stems from the velocity being aligned with the self-propulsion force, hence requiring an atypically strong noise to generate the time-reversed trajectories. Physically, the entropy production rate σ measures the (inverse) time scale over which the self-propulsion makes the trajectory irreversible: at short time scales, the translational diffusion due to Brownian motion dominates self-propulsion hence hiding the irreversible character of the dynamics; on longer time scales, translational diffusion plays a lesser

role in transport than self-propulsion, which makes the irreversibility stemming from the latter more apparent. Note that σ diverges as D goes to zero, so that the dynamics becomes strongly irreversible in this limit.

The situation is completely different if one tries to characterize the TRS breaking for the trajectory shown in Figs. 3b&d. There, only the position of the particle is measured and its original and final orientations are unknown. If the system is endowed with periodic boundary conditions, the steady state distribution is an isotropic, uniform distribution so that it is equally likely to find trajectories with $\theta(t)$ or the flipped orientation $\tilde{\theta}(t) = \pi - \theta(t)$. The entropy production thus vanishes since the time reversed of any trajectory with $\theta(t)$ can be realized with the same probability by a trajectory starting from the final position $\mathbf{r}(t_f)$ with a flipped orientation $\tilde{\theta}(t_f)$. Note that this symmetry resembles that of underdamped Langevin equations in which the time-reversal symmetry in configuration space emerges from a symmetry in phase-space upon flipping the velocities under time reversal. This parallel between active particles and underdamped passive ones has been exploited to reveal a similar symmetry of the evolution operator of AOUPs^{36,68,124}. Note that this TRS in position space is independent of the value of D and holds even for $D = 0$.

Finally, we comment on the fact that whether or not one observes TRS in active systems depends on what can be measured. Consider for example Quincke colloidal particles³¹. These particles acquire self-propulsion through the spontaneous breaking of a symmetry: their polarity stems from an asymmetric charge distribution on their surface. For an isolated particle, measuring this asymmetry or the flow of the surrounding fluid are required to distinguish a forward trajectory from a time-reversed one. In sum, in a dilute, uniform active system, the observation of a breakdown of TRS depend on the degrees of freedom which are considered. Describing the energy source^{47,147}, or considering the inertia of these typically overdamped systems¹⁶⁹, will lead to different characterization of the irreversibility of the dynamics. This strongly differs from equilibrium dynamics, in which TRS holds irrespective of the degree of coarse-graining.

The situation changes drastically when active particles are interacting with their surrounding. While an ambiguity regarding the status of TRS may remain for isolated active particles in the steady state, their interactions with external potentials or with other particles typically reveal their non-equilibrium nature, as we discuss in Sections 3 and 4.

3 Non-interacting active particles in the presence of obstacles and external potentials

Consider a system in equilibrium in which a small obstacle is introduced. The corresponding perturbation $\delta V(\mathbf{r})$ leads to a localized perturbation of the Boltzmann weight $P_{\text{eq}}(\mathbf{r}) \propto \exp[-\beta(V(\mathbf{r}) + \delta V(\mathbf{r}))]$. In that sense, the perturbation remains local. Furthermore, TRS is maintained so that even systems with asymmetric obstacles cannot harbor steady currents. Both features are challenged in active systems, whose fate in the presence of obstacles and external potentials have attracted a lot of interest^{4, 12, 18, 39, 42, 53, 57, 59, 64, 88, 89, 98–100, 121, 135, 138, 173, 186, 203} both for fundamental reasons, in that they probe the relationship between active and passive dynamics, but also for practical ones. External potentials and confinements are indeed the toolbox used to engineer and probe active systems, from optical & acoustic tweezers¹⁸⁹ to centrifuges¹⁶⁴ and arrays of obstacles⁷². In addition to a wealth of experimental works^{50, 54, 76, 77, 142, 172}, these questions have been addressed at the theoretical level by considering the overdamped dynamics

$$\dot{\mathbf{r}} = \mathbf{v}_p - \mu \nabla V(\mathbf{r}) \quad (11)$$

where the self-propulsion \mathbf{v}_p evolves either through tumbles^{4, 166, 185}, rotational diffusion^{173, 203}, or as an Ornstein-Uhlenbeck process^{68, 183}. In all cases, one can define a persistence time τ , a typical self-propulsion speed v_0 , a persistence length $\ell_p = v_0 \tau$, and a large-scale diffusivity $D_{\text{eff}} \propto \ell_p^2 / \tau$. In the limit $\tau \rightarrow 0$ keeping D_{eff} constant, the dynamics becomes equivalent to a passive one and leads to a Boltzmann distribution with an effective temperature $T_{\text{eff}} \equiv D_{\text{eff}} / \mu$. As the persistence time increases, active systems both develop non-Boltzmann features and exhibit TRS violations. We first review below the $\tau = 0$ limit before discussing the nonequilibrium static and dynamic features that develop as τ increases.

The $\tau = 0$ limit and the universal effective equilibrium regime. For AOUPs, the equilibrium behaviour stems from the fact that the Gaussian process \mathbf{v}_p becomes, as $\tau \rightarrow 0$, a white noise: $\langle v_{p,\alpha}(t)v_{p,\beta}(0) \rangle = \delta_{\alpha,\beta} \frac{D}{\tau} \exp(-\frac{|t-t'|}{\tau}) \xrightarrow{\tau \rightarrow 0} 2D\delta_{\alpha,\beta}\delta(t-t')$. The dynamics is thus equivalent to a passive one with a temperature $T_{\text{eff}} = D/\mu$. The effective equilibrium regime also exists for ABPs and RTPs, despite their non-Gaussian natures. This has been established in any dimension^{39, 173} and we detail it here for RTPs in $d = 1$. In the presence of a confining potential $V(x)$, the steady-state distribution is given by^{175, 196}:

$$P(x) = \frac{v_0^2 P_0}{v_0^2 - \mu^2 V'(x)^2} \exp \left[-\frac{\mu}{\tau} \int_0^x dx' \frac{V'(x')}{v_0^2 - \mu^2 V'(x')^2} \right], \quad (12)$$

where τ^{-1} is the tumbling rate. Note that Eq. (12) exhibits, in general, a non-Boltzmann form: the forces experienced by the particle (that do not stem from the bath) are not proportional to $\nabla \log P$.

Next, consider the $\tau \rightarrow 0$ limit, keeping $T_{\text{eff}} = \frac{v_0^2 \tau}{\mu}$ finite. This implies a large v_0 limit, so that $v_0 \gg \mu V'(x)$ for smooth potentials, which allows one to expand (12) into

$$P(x) = P_0 \exp[-V(x)/T_{\text{eff}}]. \quad (13)$$

For confining potentials, even if the condition $v_0 \gg \mu V'(x)$ cannot hold everywhere, the approximation (13) can be shown to be self-consistent if $\mu V''(x_0)\tau \ll 1$, where x_0 is the minimum of the potential, see Appendix B. These criteria generalize to $v_0 \gg \mu |\nabla V|$ and $\mu \tau \Delta V \ll 1$ in higher dimensions¹⁷³.

This effective equilibrium regime was demonstrated theoretically for sedimenting RTPs¹⁸⁶, ABPs^{59,64,89,100,173,203,212} and AOUPs¹⁸³, whose sedimentation profiles have been computed theoretically and lead to Eq. (13) in the small τ limit. Experimentally, the effective equilibrium regime has been measured for sedimenting self-propelled diffusiophoretic colloids^{76,77,142}. For ABPs, RTPs and AOUPs in harmonic traps, the effective equilibrium regimes have also been studied theoretically^{121,183,186,189} and measured in experiments¹⁸⁹. Probing effective equilibrium regimes in more general experimental settings remains an open challenge⁸⁵.

Departure from the $\tau = 0$ limit: non-Boltzmann distributions. Non-thermal effects have naturally been the focus of the community and the departure from the $\tau = 0$ limit is particularly relevant from that perspective. Despite a universal $\tau = 0$ regime, different models of self-propelled particles have been shown to lead to different behaviours, both from a static and a dynamic perspective, as soon as $\tau \neq 0$. General expressions for arbitrary potentials have been obtained for a single RTP in one dimension to any order in τ , see Eq. (12). For AOUPs, many different approaches have been developed. Some are based on calculating the steady-state directly using either path integrals^{30,130,211} or perturbative approaches^{28,68,96,128,129}. Others rely on effective equilibrium approximations of the dynamics^{35,61,69,70,93,117,127,208,209}. As a result, the steady-state distribution for N interacting AOUPs has been obtained to order τ in any dimension^{28,68,117,129}. For a single AOUP, it has been obtained explicitly up to order τ^2 using a perturbative expansion that can be extended to higher orders^{28,68,128,129}. We use these results below to illustrate and contrast the departure of the steady-state distribution from its $\tau = 0$ limit for both RTPs and AOUPs.

In both cases, the steady-state distribution in the presence of a confining potential $V(x)$ can be written, in one dimension, as in Eq. (13), albeit with $V(x)$ replaced by an effective potential

$V_{\text{eff}}(x)$, which can be computed perturbatively. For an AOUP, one finds

$$V_{\text{eff}}(x) = V(x) - \tau \left(T_{\text{eff}} V''(x) - \frac{V'(x)^2}{2} \right) - \tau^2 \left(\frac{T_{\text{eff}}^2 V^{(4)}(x)}{2} + \frac{\int^x V'(y)^2 V^{(3)}(y) dy}{2} - T_{\text{eff}} V'(x) V^{(3)}(x) - T_{\text{eff}} \frac{V''(x)}{4} \right) + \mathcal{O}(\tau^3). \quad (14)$$

A number of interesting features can already be noted in this perturbative expansion. First, a purely repulsive potential $V(x)$ may lead to an effective potential with attractive parts, due to the term $-\tau T_{\text{eff}} V''(x)$. While derived perturbatively, this gives a heuristic explanation for the accumulation of active particles close to walls, which is a trademark of active particles^{57,58,60,165,203,214}. Second, an important difference between passive and active systems can be observed at order τ^2 in Eq. (14): The steady-state distribution $P(x)$ is a non-local functional of V for active particles. Consider a dilute system. In thermal equilibrium, a perturbation of the potential δV localized at y does not impact $P(x \neq y) \propto e^{-\beta[V(x)+\delta V(x)]} = e^{-\beta V(x)}$, up to an overall normalization. In the active case, Eq. (14) reveals a completely different behaviour: $P(x \neq y)$ now depends on $V(y)$ for arbitrary large values of $|x - y|$, as exemplified in Appendix C. This is a simple heuristic explanation of remarkable experiments conducted on swimming bacteria that show an array of asymmetric obstacles to act as a pump when placed in the middle of a microfluidic cavity⁷² (See Fig. 4).

The derivation of the steady-state distribution of a single RTP can also be carried out using Eq. (12), yielding

$$V_{\text{eff}}(x) = V(x) - \frac{\mu\tau}{T_{\text{eff}}} \left((V'(x))^2 + \frac{1}{T_{\text{eff}}} \int^x dy (V'(y))^3 \right) + \mathcal{O}(\tau^2). \quad (15)$$

Again, both the emergence of effective attractive interactions out of repulsive potentials and the non-locality of $P(x)$ emerge as τ departs from 0. Contrary to AOUPs, however, both effects are already present at order τ , hence highlighting the non-universality of the departure from the $\tau = 0$ equilibrium limit across models.

Much less is known in higher dimensions, where exact results and controlled perturbative expansions are harder to get. The far-field perturbations due to localized objects have been characterized¹² and the steady-state distributions of AOUPs can be obtained perturbatively^{35,61,68–70,93,117,127,129,208,209}. Interestingly, both the effective attractions and the non-local corrections to the density field remain present. The perturbation to the density field induced by an asymmetric obstacle now decays as a dimension-dependent power-law of the distance to the object¹². These results on the impact of an asymmetric object have also been extended to active particles experiencing pairwise interactions⁸³. By contrast, in the passive case, a perturbation of the density field on the scale of the correlation

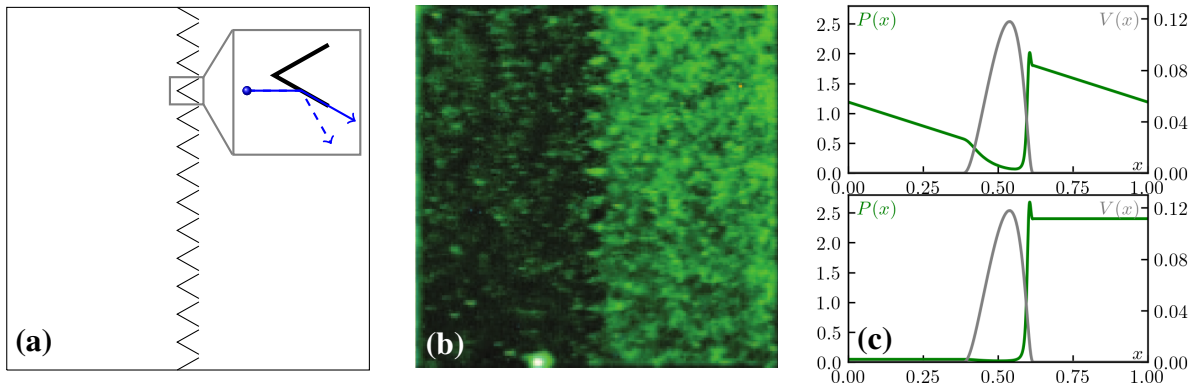


Figure 4: **(a) & (b)** Microfluidic chamber in which run-and-tumble bacteria or colloidal particles can be inserted. An array of asymmetric obstacles split the cavity into two regions **(a)**. While colloidal particles would lead to a uniform density away from the obstacles, bacteria accumulate in one side of the system **(b)**, as shown by their fluorescence signal ⁷². **Inset of (a):** The non-Boltzmann distribution solely stems from the interaction between particles and walls. Replacing the aligning torques experienced by the bacteria upon encountering a wall (solid blue line) by a specular reflection (dashed blue line) of their orientation would lead to a time-reversal symmetric dynamics and a uniform density ¹⁸⁶. The arrow of time can be read in the bacterial dynamics (solid blue line) by comparing the occurrence probability of forward and backward trajectories. The former requires no tumble to occur during a time τ whereas the latter requires a tumble to return to the original position. **(c)** Steady-state density profiles (green) generated by an asymmetric obstacle (grey) placed at the center of the system. Closed boundary conditions (bottom) lead to a density difference in the two compartments whereas periodic boundary conditions (top) lead to a linear profile away from the obstacle and a non-zero current.

length is expected. Away from criticality, these are short-range effects and hence much weaker than those found in active systems. Finally, these power-law corrections to the density field have striking consequences in the presence of a disordered potential, as exemplified by the suppression of the motility-induced phase separation ¹⁵⁸.

To illustrate the discussion above, we now come back to the examples of sedimenting and trapped active particles whose effective equilibrium regimes were discussed before. In the case of sedimenting active particles, the sedimentation profiles remain given by the Boltzmann weight in their distal region even when the condition $v_0 \gg \mu \nabla V$ does not hold: $\rho(z) \propto \exp(-\delta mgz/\lambda)$ where δmg is the effective weight of the particles and λ is a system-dependent constant that differs for AOUPs, ABPs and RTPs. For AOUPs, λ is always equal to T_{eff} ¹⁸³, even outside the small τ regime. By contrast, λ explicitly depends on δmg for ABPs and RTPs, and leads to a gravitational collapse, $\lambda = 0$, when the sedimentation speed $\mu \nabla V$ equals the self-propulsion one ¹⁸⁶. Next, we turn to the harmonic confinement of active particles ^{15,42,50,53,88,121,135,148,173,186,189}. First, results on AOUPs suggest that, as for sedimentation, the equilibrium phenomenology survives: the steady state remains a Gaussian, albeit with a potential-dependent effective temperature ¹⁸³ and the entropy production vanishes ⁶⁸. This is in stark contrast with ABPs and RTPs for which a trapping force $F(\mathbf{r}) = -k\mathbf{r}$ leads to a finite horizon $r_{\text{max}} = v_0/(\mu k)$. The Gaussian behaviour in the small τ limit is replaced by a sharp density accumulation at $r = r_{\text{max}}$ in the opposite limit ^{15,42,53,173,186,189}. It is interesting to note that AOUPs, which are praised for their simplicity, miss, in this case, an important feature of active dynamics.

Departure from the $\tau = 0$ limit: the emergence of non-equilibrium dynamical features. As discussed in the Box *Identifying time-reversal symmetry breaking*, the departure from thermal equilibrium is not only signaled by a non-Boltzmann distribution but, most importantly, by the emergence of novel dynamical features resulting from the breakdown of TRS. This can already be seen at the non-interacting level in the presence of external potentials for large enough persistence times. Some of these nonequilibrium dynamical features have recently attracted a lot of attention and are discussed below.

1. **Steady-state currents.** One of the most important results in non-equilibrium statistical mechanics is the generic emergence of steady-state currents resulting from the interplay between the breakdown of TRS and the lack of spatial symmetries. From Brownian ratchets ^{62,86,119,146,168,171} to molecular motors ^{3,92}, this has been exemplified first by considering non-equilibrium dynamics in the presence of asymmetric potentials. These results extend

to active particles, whose isotropic motions are also rectified in the presence of asymmetric potentials, leading to the emergence of steady-state currents ^{2,75,98,149,181,215}.

Analytically, the current has been computed for AOUPs ^{128,129} and RTPs ⁴ in one dimension in the presence of a periodic, asymmetric potential. Perturbatively in τ , the currents scale as τ^2 and τ for AOUPs and RTPs, respectively. This highlights, once again, the difference between these models as they depart from the effective equilibrium regime. Mathematically, it can be traced back to the order in τ at which the non-local terms appear in Eqs (14) and (15).

These results can easily be generalized to a single localized obstacle in the presence of periodic boundary conditions. In one space dimension, the current then decays as the inverse system size and a linear density profile is observed away from the obstacle (See Fig 4(c)). These results generalize to higher dimensions where asymmetric obstacles also generate currents. In the case of localized obstacles, the currents are long ranged and decay with the distance r to the object as a dimension-dependent power-law ^{12,83}: $|\mathbf{J}| \propto r^{-d}$.

The presence of a current signals a non-zero mean force exerted by the obstacle on the active fluid. By Newton's third law, a current implies a net force exerted by the fluid on the object. This explains, for instance, why an asymmetric gear immersed in a bacterial bath exhibits a persistent biased rotating motion in the steady state ^{54,118,172}. From a mechanical balance perspective, relevant in these overdamped systems, a non-zero mean current implies a non-zero drag, which has to be balanced by a net force from the object, whence relating currents and forces in active systems ^{83,138}.

The generic emergence of currents outside equilibrium when spatial symmetries are broken displays interesting exceptions. In active systems, for instance, currents are absent if, instead of using asymmetric potentials, one enforces an asymmetric spatial modulation of the self-propulsion speed ¹⁸¹, despite non-homogeneous steady-state density profiles ^{7,8,71,166,185}. The currents are, somewhat counter-intuitively, restored upon the addition of pairwise forces ¹⁸¹. This is reminiscent of the physics of passive particles in the presence of an asymmetric modulation of the temperature field where currents are only observed in the presence of interactions between particles ¹⁹⁸.

2. **Entropy production.** The computation of the entropy production rate for a non-interacting run-and-tumble particle presented in section 2 can be generalized to the case of an external force \mathbf{F} : $\dot{\mathbf{r}} = \mu \mathbf{f}_p + \mu \mathbf{F} + \sqrt{2D} \boldsymbol{\eta}$. When computing the entropy production in the full $(\mathbf{r}, \mathbf{f}_p)$ space, one then finds $D\sigma/\mu = \langle \dot{\mathbf{r}} \cdot \mathbf{f}_p \rangle + \langle \dot{\mathbf{r}} \cdot \mathbf{F} \rangle$. For a conservative force $\mathbf{F} = -\nabla V(\mathbf{r})$, this reduces to $\sigma = \frac{\mu}{D} \langle \dot{\mathbf{r}} \cdot \mathbf{f}_p \rangle = \frac{\mu}{D} w_p$. The absence of V in this second formula does not imply

an entropy production rate independent of the potential: the dissipation w_p indeed depends on $V(\mathbf{r})$ through the precise form of the steady-state distribution.

Integrating out \mathbf{f}_p to compute the entropy production rate $\tilde{\sigma}$ in \mathbf{r} -space is, however, not as easy as in the absence of external force and there is no general expression for $\tilde{\sigma}$. We simply know that coarse-graining these mesoscopic stochastic dynamics can only lower their entropy production rate so that $\tilde{\sigma} \leq \sigma$ (see, e.g., ¹⁶⁰). Progress has been made when the active noise is a Gaussian process, as is for instance the case for AOUPs. There, the computation has been carried out for N interacting particles in d dimensions, in the presence of forces stemming from a potential V , leading to ^{68, 82, 128, 129} $\sigma = \frac{\tau^2}{2D} \langle (\dot{\mathbf{r}} \cdot \nabla)^3 V(\mathbf{r}) \rangle$. This expression simplifies in the small persistence time limit to give $\sigma = \frac{D\tau^2}{2} \langle \sum_{i,j,k} (\nabla_i \nabla_j \nabla_k V)^2 \rangle$. It is remarkable that, to order τ , AOUPs are time-reversal symmetric, despite their steady-state distribution already being different from the Boltzmann weight.

3. **Activated events, non-Arrhenius law and Onsager-Machlup symmetry.** In equilibrium, an important consequence of TRS is the celebrated Onsager-Machlup symmetry ^{112, 140} which states that, in a macroscopic system (or in a small-noise limit), the most likely path to realize a rare excursion follows the time-reversal of the most likely relaxation from this rare event into the most probable state. This has important consequences, for instance, for reaction-rate theory where it implies that, in the small noise limit, transitions between states are realized by following steepest-gradient ascent and descent in a free energy landscape. This symmetry breaks down out of equilibrium, an effect that has attracted a lot of interest ^{20, 21, 187} and may lead to non-equilibrium dynamical phase transitions ^{11, 24, 25, 33}.

Apart from recent results on nucleation pathways in MIPS ^{105, 154, 156}, reaction-rate theory remains largely uncharted territory for active matter. Interesting differences with equilibrium dynamics have already been observed at the level of first-passage time computations ^{5, 30, 211}. In the low-noise regime, Arrhenius law is, for instance, not valid ²¹⁰ and the barrier crossing is controlled by a combination of force balance and potential differences.

4. **Linear response** studies the reaction of systems to small perturbations. For Markov processes, even out of equilibrium, the Agarwal formula generically predicts the response of an observable A to the perturbation of the system by a field B from the knowledge of steady-state correlations ^{1, 14, 151}. This formula also requires the knowledge of the steady-state distribution and it only reduces to the celebrated fluctuation-dissipation theorem (FDT) when the steady state is given by a Boltzmann weight. Experimentally, the FDT allows the characterization, at the microscopic scale, of passive systems using microrheological, mechanical measurements.

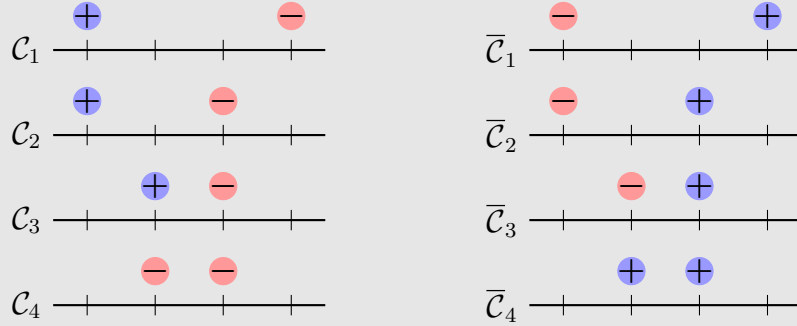
A first approach to linear response in active systems relied on measurements of ‘violations’ of the equilibrium FDT, or lack thereof. This first allows identifying regimes in which an ‘effective temperature’ can be defined^{27,45,85,104,108–110,133,173,182,183,204}. Then, the breakdown of FDT can also be used to identify the time scales over which activity drives biological systems out of equilibrium, both in vitro¹³¹ and in vivo^{26,65–67,84,159,205}. An alternative approach is to start from a microscopic model of active systems and explicitly construct its linear response¹¹⁴. This has, in particular, been carried out using perturbative expansions^{41,68,129} or Markovian approximations^{37,49} and might pave the way towards a systematic microrheology of active systems.

4 TRS in the presence of interactions in active systems

One of the most striking features of active systems is the wealth of dynamical phenomena it exhibits that are without counterparts in equilibrium. From the emergence of travelling waves in colloidal rollers³¹ to the collective migration of cell monolayers¹⁵⁰, a trademark of active systems is the emergence of macroscopic steady-state currents (See Fig. 1). This is a clear TRS-breaking, non-equilibrium feature that allows to immediately distinguish active from passive systems in many situations. Mechanistically, as exemplified by the physics of flocking^{194,201}, this naturally emerges in phase transitions whose order parameters are coupled to the particle orientations. Estimating the entropy production rate in these strongly irreversible systems is an open problem, on which progress has been made recently using field-theoretical descriptions of flocking models²⁹. Note that, while the global phenomenology of a model can be strongly out of equilibrium some of its features may retain an equilibrium nature, as was for instance suggested for angular correlations between birds in starling flocks¹³². Identifying the degrees of freedom that contribute to TRS violations is thus also an open challenge^{16,78,129,134}.

Microscopically, the breakdown of TRS emerges from very simple interactions between particles, even without relying on alignment. Indeed, mutual hard-core exclusion suffices to make active dynamics irreversible¹²² (See Box *Violation of TRS resulting from hard-core interactions* for a simple example). A natural question is then whether TRS survives in some classes of interacting active-matter systems. We discuss below two such instances. First, we consider MIPS in which TRS is partially restored by coarse-graining in certain classes of systems. We then discuss under which conditions coarse-graining may restore TRS exactly, considering in particular tactic systems. Finally, we turn to the small-persistence-time regime in which an exact TRS is recovered for interacting AOUPs despite a non-Boltzmann distribution.

Violation of TRS resulting from hard-core interactions. Consider the following one-dimensional lattice model of run-and-tumble particles^{122,179,191}: \oplus and \ominus particles hop to the right and to the left at rate p on empty sites, respectively. In addition, particles change direction at a rate α . Consider the sequence of configuration \mathcal{C}_1 to \mathcal{C}_4 :



Starting from \mathcal{C}_1 at $t = 0$, let us call t_i the transition times from \mathcal{C}_i to \mathcal{C}_{i+1} . Denoting $i_{1,2}, \sigma_{1,2}$ the positions and signs of both particles, the probability density to observe this trajectory during $[0, t_f]$ is given by

$$P[i_{1,2}(t), \sigma_{1,2}(t)] = e^{-2(p+\alpha)t_1} p \times e^{-2(p+\alpha)(t_2-t_1)} p \times e^{-2\alpha(t_3-t_2)} \alpha \times e^{-(p+2\alpha)(t_f-t_3)}. \quad (16)$$

The first three factors correspond to the transition \mathcal{C}_i to \mathcal{C}_{i+1} with $i = 1, 2, 3$ whereas the last factor is the probability of staying in \mathcal{C}_4 up to t_f . The probability to observe the reverse trajectories $P[i_{1,2}(t_f - t), \sigma_{1,2}(t_f - t)]$ trivially vanishes: a \oplus particles cannot hop backwards in this model, nor can a \ominus hop forward. More interestingly, one may wonder whether reversibility survives if only the positions of the particles are recorded. The converse sequence of positions could indeed be realized by flipping the orientations of the particles (using a so-called kinematic reversibility¹²²). This corresponds to the sequence $\bar{\mathcal{C}}_4$ to $\bar{\mathcal{C}}_1$ described above. The probability density of this trajectory can also be evaluated, yielding

$$P[i_{1,2}(t_f - t), -\sigma_{1,2}(t_f - t)] = e^{-(p+2\alpha)(t_f-t_3)} \alpha \times e^{-2(p+\alpha)(t_3-t_2)} p \times e^{-2(p+\alpha)(t_2-t_1)} p \times e^{-2(p+\alpha)t_1} \quad (17)$$

Interestingly, the probability densities (16) and (17) are unequal, showing the system to lack TRS in position space at the level of individual trajectories. By comparing the various terms, the irreversibility is seen to stem from the different rates at which the system hops out of configurations \mathcal{C}_3 and $\bar{\mathcal{C}}_3$ (2α and $2\alpha + 2p$, respectively). These different escape rates lead to the factors $e^{-2(p+\alpha)(t_3-t_2)}$ and $e^{-2\alpha(t_3-t_2)}$, which are the sole terms violating TRS. If typical trajectories include an extensive number of collisions in time, this will lead to a non-zero entropy production

rate. All in all, it is thus the interaction between the particles which generates the violation of TRS, as first explained in ¹²².

TRS and effective equilibrium descriptions of MIPS. Consider an equilibrium system comprising Brownian particles interacting via a pairwise potential made of a hard core and a soft attractive tail. The steady state of the system is found by balancing entropy, which favors disordered configurations, with energy. At moderate densities, the latter favors cohesion thanks to the attractive part of the potential. As the temperature is lowered, energy wins over entropy and a gas-to-liquid phase transition is observed. When the total number of particles is conserved, this leads to phase coexistence. Now, make the particle active. A natural way to preserve phase separation is to make self-propulsion weak enough that it does not overcome the attractive interactions. Interestingly, however, the largest part of the phase diagram exhibiting liquid-gas coexistence is not found at small self-propulsion speeds but at large ones ¹⁵², and it is observed even in the absence of any attractive tail ^{63,153} (See Fig. 5). A cohesive phase may thus emerge out of purely repulsive pairwise forces in active systems. This phase-separated state cannot be accounted for using the Boltzmann weight and is a trademark of active particles. It results from a motility-induced phase separation ⁴⁰ through which particles whose self propulsion is hindered at high density separate between a dense, almost arrested, phase and a dilute active gas.

Despite its non-Boltzmann nature, the dynamics of such a phase-separated system at the macroscopic scale, however, does not reveal any clear breakdown of TRS at first sight, and the difference with an equilibrium phase separation is hard to pinpoint. Therefore, many ideas based on equilibrium theories have been proposed to account for MIPS ^{144,145,154,176,177,180,185,188}. Below we first focus on large-scale TRS violations in MIPS before discussing when and how a generalization of equilibrium approaches may be used to describe MIPS and other phase transitions.

Large-scale TRS violations in MIPS. We now focus on the MIPS observed in systems with quorum-sensing interactions, i.e. when the speed of a particle explicitly depends on the local density of particles around it ^{17,102,185}:

$$\dot{\mathbf{r}}_i = v(\mathbf{r}_i, [\rho])\mathbf{u}_i, \quad \rho(\mathbf{r}) \equiv \sum_i \delta(\mathbf{r} - \mathbf{r}_i), \quad (18)$$

where \mathbf{u}_i undergoes either rotational diffusion or instantaneous Poisson-distributed tumbles. A common form for $v(\mathbf{r}_i, [\rho])$ is then ^{173,176}

$$v(\mathbf{r}_i, [\rho]) = f[\tilde{\rho}(\mathbf{r}, t)], \quad \tilde{\rho}(\mathbf{r}, t) \equiv \int d\mathbf{r}' \rho(\mathbf{r}') K(\mathbf{r}_i - \mathbf{r}'), \quad (19)$$

where K is a kernel which can stem from integrating out the signal used by the particles to communicate ¹⁴¹, and f determines how the particles react to their peers. Equations (18) and (19), together with $K(\mathbf{r}) = \delta(\mathbf{r})$ and f a linearly decaying function, have been proposed as a toy model for systems with pairwise repulsive forces ^{23,191}, even though the latter offer a richer phenomenology such as hexatic order ^{9,55,94} or bubbly phases ^{170,193}.

A glimpse into the large-scale behaviour of this system can be obtained using a diffusive approximation on Eq. (18), which leads to the fluctuating hydrodynamics ^{120,173,176}

$$\dot{\rho} = \nabla \cdot [\rho D \nabla \mu + \sqrt{2\rho D} \Lambda] \quad \text{with} \quad D = \frac{v^2 \tau}{d} \quad \text{and} \quad \mu = \log \rho + \log f(\tilde{\rho}), \quad (20)$$

where Λ is a Gaussian white-noise field of zero mean and correlations $\langle \Lambda_\alpha(\mathbf{r}, t) \Lambda_\beta(\mathbf{r}', t') \rangle = \delta_{\alpha\beta} \delta(\mathbf{r} - \mathbf{r}') \delta(t - t')$ and d is the number of space dimensions. By analogy to the equilibrium model B , we refer to μ as a chemical potential. The dynamics (20) satisfies TRS if and only if $\mu(\mathbf{r})$ is a gradient of a free-energy functional ¹⁷³. This holds when a generalization of the Schwarz equality to functional derivatives is obeyed:

$$\frac{\delta \mu(\mathbf{r}, [\rho])}{\delta \rho(\mathbf{r}')} = \frac{\delta \mu(\mathbf{r}', [\rho])}{\delta \rho(\mathbf{r})}, \quad (21)$$

where the equality is understood as between distributions ¹⁴¹.

For a generic $f(\tilde{\rho})$, Eq. (21) is not satisfied and the dynamics (20) does not obey TRS. An interesting exception is when $K(\mathbf{r}) = \delta(\mathbf{r})$; v is then a local function of the density and Eq. (20) satisfies an exact TRS ¹⁸⁵. For more general kernels, a free-energy functional is only found for $f(\tilde{\rho}) = v_0 \exp(-\lambda \tilde{\rho})$ ⁸². When this is not the case, it is interesting to see which features of the dynamics are directly responsible for breaking TRS. To do this, we can expand μ to second order in gradients:

$$\mu[\mathbf{r}] = \log \rho + \log f(\rho) - \kappa \Delta \rho \quad \text{where} \quad \kappa(\rho) = -\ell^2 \frac{f'(\rho)}{f(\rho)}, \quad (22)$$

and $\ell^2 = \int d\mathbf{r}' K(\mathbf{r}) \mathbf{r}'^2$ is a measure of the interaction range ¹⁷⁶. The entropy production rate can then be computed using methods akin to those presented in ¹³⁴ as:

$$\sigma = - \lim_{t \rightarrow \infty} \frac{1}{2t} \int_0^t ds \int d\mathbf{r} \dot{\rho}(\mathbf{r}, t) \kappa[\rho(\mathbf{r}, t)] \Delta \rho + \mathcal{O}(\nabla^4) \simeq \frac{1}{2} \int d\mathbf{r} \langle \dot{\rho}(\mathbf{r}) \kappa[\rho(\mathbf{r})] \Delta \rho \rangle, \quad (23)$$

where the last equality stems from ergodicity. A few comments are in order. First, a completely local approximation to μ , that neglects all gradient terms, leads to a vanishing entropy production rate. This is consistent with the apparent macroscopic similarity between MIPS and an equilibrium liquid-gas separation. Then, taking gradients into account, TRS is broken and Eq. (23) offers a spatial decomposition of the entropy production rate. It suggests that the latter is most pronounced in inhomogeneous regions, namely next to interfaces between coexisting phases. Figure 5 shows a measure of σ in a simplified version of the field-theory (20) undergoing MIPS, which is commonly referred to as active model B. The entropy production rate is indeed peaked at the interface between the gas and liquid phases, a result that was confirmed using microscopic simulations of AOUPs ¹²⁹. This role of interfaces in TRS breakdown also has consequences for static properties, as exemplified by the construction of the phase diagram which we now discuss.

Phase diagram and generalized thermodynamics of MIPS. A natural question is whether the dynamical differences between MIPS and an equilibrium phase separation also affect the static properties, and in particular the density profiles connecting coexisting phases which, as we discuss below, determine the phase diagram. The simplest way of answering this question is to take a mean-field approximation. In a homogeneous system, we can use a local approximation of μ , defined in Eq. (20), to obtain the Landau free energy $\mathcal{F} = \int d\mathbf{r} \phi[\rho(\mathbf{r})]$, where $\phi(\rho) = \rho(\log \rho - 1) + F(\rho)$ with $F'(\rho) = \ln f(\rho)$. The linear stability of a homogeneous phase at density ρ_0 is then lost whenever $\phi''(\rho_0) < 0$, i.e. $\rho_0 f'(\rho_0) < -f(\rho_0)$. This defines a spinodal region within which the system is linearly unstable to MIPS ¹⁸⁵. At this level, there is no difference with an equilibrium mean-field theory. To account for the resulting phase-separated state, it is necessary to consider inhomogeneous profiles.

To do so, we again use the leading-order gradient expansion of μ given by Eq. (22). At this level, the mapping to equilibrium is violated and equation (21) is not satisfied. (Again, an exception occurs for $f(\tilde{\rho}) = v_0 \exp(-\lambda\tilde{\rho})$ ¹⁸⁵.) The attempts ^{180,185,188} to build the phase diagram using common-tangent constructions on $\Phi(\mathbf{r})$ are thus bound to fail ^{174,207}. Somewhat surprisingly, if $\mu(\mathbf{r})$ cannot be written as the functional derivative of a free energy with respect to $\rho(\mathbf{r})$, a gradient form can be found upon a change of variable $\rho \rightarrow R(\rho)$, where $R'(\rho) = 1/\kappa(\rho)$. Then, $\mu(\mathbf{r}) = \nabla \frac{\delta \mathcal{H}}{\delta R(\mathbf{r})}$, where $\mathcal{H} = \int d\mathbf{r} [\Phi(R) + \frac{\kappa}{2R'} (\nabla R)^2]$ and $\Phi'(R) = \log \rho(R) + \log f(\rho(R))$. This allows identifying μ and a generalized pressure $P \equiv R \frac{d\Phi}{dR} - \Phi$ as state variables, which are equal in coexisting phases ^{176,177}. Equivalently, a common-tangent construction on $\Phi(R)$ can be used to construct the coexisting densities. Despite its mean-field nature, this construction was shown to

give precise estimates of the phase diagram for microscopic models of quorum-sensing active particles undergoing MIPS, without any fitting parameters^{176,177} (See Fig 5). Note that the agreement does not extend up to the putative critical point close to which the mean-field theory is expected to break-down in a Ginzburg interval (which is not numerically resolved). Furthermore, at large propulsion speeds, domain walls become so sharp that higher-order gradients cannot be neglected leading to quantitative differences with the predictions of (22).

Tactic dynamics. In the case of MIPS, the strong TRS violations exhibited at the single particle level (σ is infinite in the absence of translational diffusion) are thus partially erased upon coarse-graining. TRS violations, occurring mostly at interfaces, survive because condition (21) is generically not satisfied. A natural question is then whether there exist active systems whose fluctuating hydrodynamics satisfy the integrability condition (21). This question was answered for tactic dynamics, in which particles move according to Eq. (8) and whose orientations \mathbf{u}_i perform tumbles at rate α and diffuse with rotational diffusivity Γ . Taxis is implemented by coupling self propulsion with the gradient of a field $c(\mathbf{r})$ through^{120,141,163}

$$v_p = v_0 - v_1 \mathbf{u}_i \cdot \nabla c \quad \alpha = \alpha_0 + \alpha_1 \mathbf{u}_i \cdot \nabla c \quad \Gamma = \Gamma_0 + \Gamma_1 \mathbf{u}_i \cdot \nabla c \quad (24)$$

The field $c(\mathbf{r})$ can be either externally imposed or, more interestingly, can be a functional of the particle density. Under the hypothesis that the large-scale diffusive scaling of non-interacting active particles survives the addition of interactions, the fluctuating hydrodynamics of this model can be constructed and Eq. (21) can be satisfied in a number of non-trivial cases¹⁴¹. In particular, when $c(\mathbf{r})$ is a diffusive signalling field produced by the particles, this system models swimming bacteria interacting via chemotaxis. The integrability of the large-scale dynamics then reveals a mapping between bacteria interacting both via chemotactant and chemorepellent and Brownian colloids interacting via attractive and repulsive forces. While the model violates TRS at the microscopic scale, the latter is restored upon coarse-graining and the rich phase diagram of this system can be accounted for exactly using equilibrium theories. Note that the fate of TRS at the fluctuating hydrodynamic level in active systems is an open, non-trivial question. For instance, another model of tactic dynamics defined as $\dot{\mathbf{r}}_i = \nu_1 \nabla c + \nu_2 (\mathbf{u}(\theta) \cdot \nabla) \nabla c$ was shown to lead to a violation of TRS at the coarse-grained level¹²⁰. The results of¹⁴¹ thus establish a non-trivial embedding of equilibrium physics in active matter systems, but slight perturbations, albeit leading to minor modifications of large-scale behaviours, may trigger TRS violations.

Small τ regime. Finally, let us mention that the equilibrium regime recovered in the $\tau \rightarrow 0$ limit while keeping $kT_{\text{eff}} = v_0^2 \tau / \mu$ constant discussed for the single-particle case survives under the addition of pairwise forces. The departure from this limiting case has been studied analytically

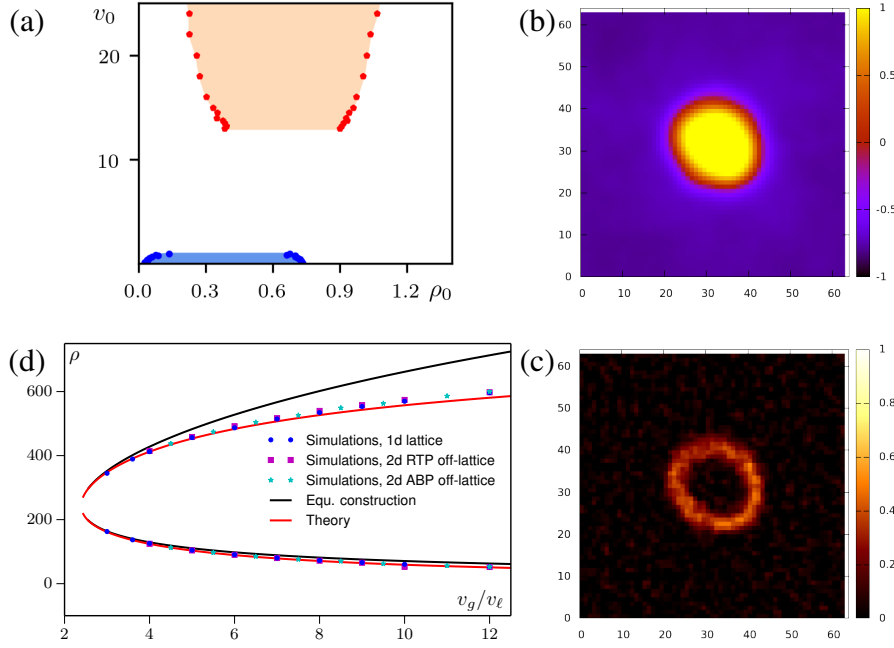


Figure 5: **(a)** Phase diagram of ABPs interacting via a Lennard-Jones potential. For vanishing self-propulsion v_0 , the system is effectively in equilibrium and undergoes a traditional liquid-gas phase separation. The phase-separated (blue) region survives at small v_0 until the self-propulsion is strong enough to overcome attractive interactions, hence vaporising the liquid phase. A reentrance into a phase-separated (orange) region is observed at larger v_0 . The latter stems from a motility-induced phase separation and would also be observed in the absence of the attractive tail of the pair potential. Symbols correspond to binodals measured in simulations of self-propelled particles interacting via a Lennard-Jones potential. The phase-separated regions are estimated numerically up to unresolved critical regions using a methodology described in Appendix D. **(b) & (c)** Simulations of a scalar field-theory undergoing motility-induced phase separation. The order parameter $\Phi(x, y)$ shown in panel (b) distinguishes a liquid phase ($\Phi = 1$) from a gas one ($\Phi = -1$). The entropy production rate can be decomposed spatially as $\sigma = \int d^2\mathbf{r} \hat{\sigma}(\mathbf{r})$. The plot of $\hat{\sigma}(\mathbf{r})$ in panel (c) shows the interface to contribute most to the TRS violations measured by σ . Adapted from ¹³⁴. **(d)** Phase diagrams of microscopic models of quorum-sensing active particles (symbols). Equating the generalized pressures P and chemical potentials μ in coexisting phases lead to a theoretical prediction (red line) in quantitative agreement with microscopic simulations. An equilibrium construction based on a local approximation of μ (black solid line) is quantitatively incorrect. Adapted from ¹⁷⁶.

for AOUPs, both using Markovian approximations^{208,209} and an explicit small- τ expansion^{68,129}. To linear order in τ , the system satisfies detailed balance with a non-Boltzmann form. Casting $\ln P$ into an effective potential, pairwise repulsive forces lead to effective attractive interactions⁶¹. While the latter do not allow to quantitatively account for MIPS¹⁵⁵, they qualitatively capture how self-propulsion turns repulsive forces into attractive ones. Finally, note that *bona fide* equilibrium systems can be studied under the perturbation of a small self-propulsion velocity, which allows studying the fate of thermodynamical concepts like surface tension or chemical potential in weakly active systems^{144,145}. The same applies to equilibrium phases, like the hexatic phase observed in 2D melting, which has been shown to survive activity^{55,94,95}.

5 Perspectives

Most active-matter models such as Eq. (1) aim at modelling the effective dynamics of self-propelled particles and not the irreversible consumption of energy powering the propulsion force. As such, they are unable to account for all the dissipative processes occurring in the system, hence rendering the theoretical assessment of its full irreversibility a somewhat hopeless endeavour. This highlights an important property of nonequilibrium systems: irreversibility depends on the degrees of freedom under study and on the scale of their description. This raises the question of the scale at which dissipation is maximal. It also opens up the possibility that equilibrium statistics prove relevant to describe specific scales or observables. Effective-equilibrium descriptions have indeed proven successful in qualitatively accounting for part of active matter phenomenology such as the motility-induced phase separation. On the contrary, time is now ripe for the identification of TRS-violating emerging behaviours and for the quantification of entropy-production rates in active pattern-forming systems. In turn, the connection between entropy production rates and more directly accessible observables such as steady-state currents remains an open challenge at the coarse-grained scale. These questions are particularly relevant in the biophysical context that gave birth to the field of active matter: cells are constantly dissipating energy to exert biological functions; assessing which of them genuinely rely on nonequilibrium processes is a fascinating open challenge.

Beyond the violation of TRS observed in active systems, we have reviewed their most salient non-Boltzmann features. That the steady-state distributions are not captured by the Boltzmann weight indeed allows for phenomenologies unmatched in passive systems, but it also impairs our ability to design smart active materials. An important challenge facing the community is then to develop alternatives to equilibrium thermodynamics that would grant us the same level of intuition

and control over active systems as we have over passive ones. Natural starting points are then the various limits in which effective equilibrium concepts can be proven relevant. From the small-but-non-zero persistence-time limit, to emerging TRS restored by coarse-graining, to the identification of state functions, we have reviewed cases in which efforts were rewarded. Beyond these cases, this calls for an extensive exploration of the fate of thermodynamic state variables (entropy, chemical potentials, *etc.*). At the local level, inferring effective interactions by means of rapidly developing learning algorithms seems a promising avenue ^{13,43,44,195}.

Acknowledgment: JO, JT, FvW acknowledge support from ANR grant THEMA; YK acknowledges support from the ISF and from an NSF-BSF grant. We thank Massimo Pica Ciamarra and Yanwei Li for sharing the data published in ¹⁰⁶ that were used to calibrate the simulations shown in Fig. 5a. The authors benefited from participation in the 2020 KITP program on Active Matter supported by the Grant NSF PHY-1748958.

A Entropy production

The forward trajectory $\mathbf{r}(t)$ and $\theta(t)$ uniquely characterize the realization of the noise through

$$\boldsymbol{\eta}(t) = \frac{\dot{\mathbf{r}}(t) - v_0 \mathbf{u}(\theta(t))}{\sqrt{2D}} \quad (25)$$

For the reversed trajectory $\mathbf{r}^r(t) = \mathbf{r}(t_f - t)$, $\theta^r(t) = \theta(t_f - t)$ to be observed, the surrounding fluid molecules have to produce a different noise

$$\boldsymbol{\eta}^r(t) = \frac{\dot{\mathbf{r}}^r(t) - v_0 \mathbf{u}(\theta^r(t))}{\sqrt{2D}} = \frac{-\dot{\mathbf{r}}(t_f - t) - v_0 \mathbf{u}(\theta(t_f - t))}{\sqrt{2D}} = -\boldsymbol{\eta}(t_f - t) - \frac{2v_0 \mathbf{u}(\theta(t_f - t))}{\sqrt{2D}} \quad (26)$$

To characterize the irreversibility of the process it is useful to note that the probability of a trajectory is given by its Onsager-Machlup form ^{140,210}

$$P[\{\mathbf{r}(t), \theta(t)\}] = Z^{-1} P[\{\theta(t)\}|\theta_0] \exp \left[-\frac{1}{4D} \int_0^{t_f} dt [\dot{\mathbf{r}}(t) - v_0 \mathbf{u}(\theta)]^2 \right] P_0(\mathbf{r}_0, \theta_0) \quad (27)$$

where $P[\{\theta(t)\}|\theta_0]$ is the probability of the realization of $\theta(t)$ starting from θ_0 , P_0 is the probability of the initial condition, and Z^{-1} is a normalization. Note that, for fully randomizing tumbles, $P[\{\theta(t_f - t)\}|\theta_f] = P[\{\theta(t)\}|\theta_0]$. Taking the logarithm of the ratio between forward and backward trajectories yield the corresponding ‘path-wise entropy production’ ¹⁶⁷:

$$\hat{\Sigma}[\{\mathbf{r}(t), \theta(t)\}] \equiv \log \frac{P[\{\mathbf{r}(t), \theta(t)\}]}{P[\{\mathbf{r}(t_f - t), \theta(t_f - t)\}]} = \frac{\mu}{D} \int_0^{t_f} dt \dot{\mathbf{r}} \cdot \mathbf{f}_p + \log \frac{P_0(\mathbf{r}_0, \theta_0)}{P_f(\mathbf{r}_f, \theta_f)}, \quad (28)$$

where $P_f(\mathbf{r}_f, \theta_f)$ is the probability of being at $\mathbf{r}_f \equiv \mathbf{r}(t_f)$ and $\theta_f \equiv \theta(t_f)$ given that the initial condition was sampled according to P_0 .

B Self-consistency of the effective temperature regime

Let us consider the self-consistency of Eq. (13) in the presence of a confining potential. Close to the minimum x_0 of the potential, the condition $v_0 \gg \mu V'(x)$ trivially holds. Let us expand the distribution (13) around x_0 . It is then given by a locally Gaussian distribution

$$P(x) \sim \exp \left[-\frac{V''(x_0)(x - x_0)^2}{2T_{\text{eff}}} \right] \quad (29)$$

This predicts a typical displacement $x_t \sim \sqrt{T_{\text{eff}}/V''(x_0)}$ which in turn leads to a typical force that scales as $V'(x_t) \simeq \sqrt{\frac{\tau v_0^2 V''(x_0)}{\mu}}$, where we have used $T_{\text{eff}} = v_0^2 \tau / \mu$. The condition $v_0 \gg \mu V'(x)$ then becomes $\mu V''(x_0) \tau \ll 1$: the typical time between two tumbles has to be much shorter than the relaxation time inside the potential well.

C Non-locality of the steady-state distribution

Consider the effective potential given in Eq. (14). Its non-local nature becomes apparent if one adds a localized perturbation $\delta V(x) = \epsilon \delta(x - y)$, centered around y , to the potential $V(x)$. The effective potential $V_{\text{eff}}(x)$ then picks up a contribution due to δV , because of the term $\frac{\int^x V'(y)^2 V^{(3)}(y) dy}{2}$. To linear order in ϵ , it reads

$$\delta V_{\text{eff}}(x) = \frac{\epsilon \tau^2}{2} [(V'(y)^2)^{(3)} + 2V''(y)V^{(3)}(y) + 2V'(y)V^{(4)}(y)] \Theta(x - y), \quad (30)$$

which adds a global step to the density profile at $x = y$.

D Self-propelled ABPs interacting via a Lennard-Jones potential

We consider N active Brownian particles evolving in two space dimensions under the dynamics:

$$\dot{\mathbf{r}}_i = v_0 \mathbf{u}(\theta_i) - \sum_j \nabla V(\mathbf{r}_i - \mathbf{r}_j) + \sqrt{2D_t} \boldsymbol{\eta}_i \quad \dot{\theta}_i = \sqrt{2D_r} \xi_i \quad (31)$$

where $\boldsymbol{\eta}_i$ and ξ_i are independent Gaussian white noises, and V is the Lennard-Jones potential

$$V(\mathbf{r}) = 4\epsilon \left(\frac{\sigma^{12}}{\mathbf{r}^{12}} - \frac{\sigma^6}{\mathbf{r}^6} \right). \quad (32)$$

Interactions between particles are truncated at $|\mathbf{r}| = 2.7\sigma$ and we used periodic boundary conditions. Figure 5a was obtained using $\sigma = 0.37$, $T = 0.4$ and $D_r = 2$. The phase-separated regions were found by running simulations for $\rho_0 = 2.5\sigma^2$ ($v_0 < 8$) and $\rho_0 = 4\sigma^2$ ($v_0 > 8$) in systems of line sizes $L = 80$ up to $t = 2000$, where ρ_0 is the rescaled number density $\rho_0 \equiv N\sigma^2/L^2$. The symbols correspond to estimates of the coexisting densities. The latter were obtained from the local maxima of histograms of the density field, constructed using bins of linear size 4.

1. Girish Saran Agarwal. Fluctuation-dissipation theorems for systems in non-thermal equilibrium and applications. *Zeitschrift für Physik A Hadrons and nuclei*, 252(1):25–38, 1972.
2. Bao-quan Ai, Qiu-yan Chen, Ya-feng He, Feng-guo Li, and Wei-rong Zhong. Rectification and diffusion of self-propelled particles in a two-dimensional corrugated channel. *Physical Review E*, 88(6):062129, 2013.
3. Armand Ajdari and Jacques Prost. Mouvement induit par un potentiel périodique de basse symétrie: diélectrophorese pulsée. *Comptes rendus de l'Académie des sciences. Série 2, Mécanique, Physique, Chimie, Sciences de l'univers, Sciences de la Terre*, 315(13):1635–1639, 1992.
4. L Angelani, A Costanzo, and R Di Leonardo. Active ratchets. *EPL (Europhysics Letters)*, 96(6):68002, 2011.
5. L Angelani, R Di Leonardo, and M Paoluzzi. First-passage time of run-and-tumble particles. *The European Physical Journal E*, 37(7):59, 2014.
6. Juan Luis Aragonés, Joshua Paul Steimel, and A Alexander-Katz. Elasticity-induced force reversal between active spinning particles in dense passive media. *Nature communications*, 7(1):1–9, 2016.
7. Jochen Arlt, Vincent A Martinez, Angela Dawson, Teuta Pilizota, and Wilson CK Poon. Painting with light-powered bacteria. *Nature communications*, 9(1):1–7, 2018.
8. Jochen Arlt, Vincent A Martinez, Angela Dawson, Teuta Pilizota, and Wilson CK Poon. Dynamics-dependent density distribution in active suspensions. *Nature communications*, 10(1):1–7, 2019.
9. Thibaut Arnoult de Pirey, Gustavo Lozano, and Frédéric van Wijland. Active hard spheres in infinitely many dimensions. *Physical review letters*, 123(26):260602, 2019.

10. Alessandro Attanasi, Andrea Cavagna, Lorenzo Del Castello, Irene Giardina, Tomas S Grigera, Asja Jelić, Stefania Melillo, Leonardo Parisi, Oliver Pohl, Edward Shen, et al. Information transfer and behavioural inertia in starling flocks. *Nature physics*, 10(9):691–696, 2014.
11. Yongjoo Baek and Yariv Kafri. Singularities in large deviation functions. *Journal of Statistical Mechanics: Theory and Experiment*, 2015(8):P08026, 2015.
12. Yongjoo Baek, Alexandre P Solon, Xinpeng Xu, Nikolai Nikola, and Yariv Kafri. Generic long-range interactions between passive bodies in an active fluid. *Physical review letters*, 120(5):058002, 2018.
13. Saientan Bag and Rituparno Mandal. Interaction from structure using machine learning: in and out of equilibrium. *arXiv preprint arXiv:2012.13330*, 2020.
14. Marco Baiesi and Christian Maes. An update on the nonequilibrium linear response. *New Journal of Physics*, 15(1):013004, 2013.
15. Urna Basu, Satya N Majumdar, Alberto Rosso, Sanjib Sabhapandit, and Grégory Schehr. Exact stationary state of a run-and-tumble particle with three internal states in a harmonic trap. *Journal of Physics A: Mathematical and Theoretical*, 53(9):09LT01, 2020.
16. Christopher Battle, Chase P. Broedersz, Nikta Fakhri, Veikko F. Geyer, Jonathon Howard, Christoph F. Schmidt, and Fred C. MacKintosh. Broken detailed balance at mesoscopic scales in active biological systems. *Science*, 352(6285):604–607, 2016.
17. Tobias Bäuerle, Andreas Fischer, Thomas Speck, and Clemens Bechinger. Self-organization of active particles by quorum sensing rules. *Nature communications*, 9(1):1–8, 2018.
18. Clemens Bechinger, Roberto Di Leonardo, Hartmut Löwen, Charles Reichhardt, Giorgio Volpe, and Giovanni Volpe. Active particles in complex and crowded environments. *Reviews of Modern Physics*, 88(4):045006, 2016.
19. Howard C Berg. *E. coli in Motion*. Springer Science & Business Media, 2008.
20. Lorenzo Bertini, Alberto De Sole, Davide Gabrielli, Giovanni Jona-Lasinio, and Claudio Landim. Macroscopic fluctuation theory for stationary non-equilibrium states. *Journal of Statistical Physics*, 107(3-4):635–675, 2002.
21. Lorenzo Bertini, Alberto De Sole, Davide Gabrielli, Giovanni Jona-Lasinio, and Claudio Landim. Macroscopic fluctuation theory. *Reviews of Modern Physics*, 87(2):593, 2015.

22. William Bialek, Andrea Cavagna, Irene Giardina, Thierry Mora, Edmondo Silvestri, Massimiliano Viale, and Aleksandra M Walczak. Statistical mechanics for natural flocks of birds. *Proceedings of the National Academy of Sciences*, 109(13):4786–4791, 2012.
23. Julian Bialké, Hartmut Löwen, and Thomas Speck. Microscopic theory for the phase separation of self-propelled repulsive disks. *EPL (Europhysics Letters)*, 103(3):30008, 2013.
24. T Bodineau, B Derrida, V Lecomte, and F Van Wijland. Long range correlations and phase transitions in non-equilibrium diffusive systems. *Journal of Statistical Physics*, 133(6):1013–1031, 2008.
25. Thierry Bodineau and Bernard Derrida. Distribution of current in nonequilibrium diffusive systems and phase transitions. *Physical Review E*, 72(6):066110, 2005.
26. P Bohec, J Tailleur, F van Wijland, A Richert, and F Gallet. Distribution of active forces in the cell cortex. *Soft matter*, 15(35):6952–6966, 2019.
27. Pierre Bohec, François Gallet, Christian Maes, Soghra Safaverdi, Paolo Visco, and Frédéric Van Wijland. Probing active forces via a fluctuation-dissipation relation: Application to living cells. *EPL (Europhysics Letters)*, 102(5):50005, 2013.
28. Luis L Bonilla. Active ornstein-uhlenbeck particles. *Physical Review E*, 100(2):022601, 2019.
29. Øyvind L Borthne, Étienne Fodor, and Michael E Cates. Time-reversal symmetry violations and entropy production in field theories of polar active matter. *New Journal of Physics*, 22(12):123012, 2020.
30. AJ Bray, AJ McKane, and TJ Newman. Path integrals and non-markov processes. ii. escape rates and stationary distributions in the weak-noise limit. *Physical Review A*, 41(2):657, 1990.
31. Antoine Bricard, Jean-Baptiste Caussin, Nicolas Desreumaux, Olivier Dauchot, and Denis Bartolo. Emergence of macroscopic directed motion in populations of motile colloids. *Nature*, 503(7474):95–98, 2013.
32. Allan M Brooks, Mykola Tasinkevych, Syeda Sabrina, Darrell Velegol, Ayusman Sen, and Kyle JM Bishop. Shape-directed rotation of homogeneous micromotors via catalytic self-electrophoresis. *Nature communications*, 10(1):1–9, 2019.

33. Guy Bunin, Yariv Kafri, and Daniel Podolsky. Cusp singularities in boundary-driven diffusive systems. *Journal of Statistical Physics*, 152(1):112–135, 2013.
34. Francesco Cagnetta, Federico Corberi, Giuseppe Gonnella, and Antonio Suma. Large fluctuations and dynamic phase transition in a system of self-propelled particles. *Physical review letters*, 119(15):158002, 2017.
35. Li Cao, Da-jin Wu, and Xue-li Luo. Effects of saturation in the transient process of a dye laser. iii. the case of colored noise with large and small correlation time. *Phys. Rev. A*, 47:57–70, 1993.
36. Lorenzo Caprini, Umberto Marini Bettolo Marconi, Andrea Puglisi, and Angelo Vulpiani. Comment on “entropy production and fluctuation theorems for active matter”. *Physical review letters*, 121(13):139801, 2018.
37. Lorenzo Caprini, Umberto Marini Bettolo Marconi, and Angelo Vulpiani. Linear response and correlation of a self-propelled particle in the presence of external fields. *Journal of Statistical Mechanics: Theory and Experiment*, 2018(3):033203, 2018.
38. Michael E Cates. Diffusive transport without detailed balance in motile bacteria: does microbiology need statistical physics? *Reports on Progress in Physics*, 75(4):042601, 2012.
39. Michael E Cates and Julien Tailleur. When are active brownian particles and run-and-tumble particles equivalent? consequences for motility-induced phase separation. *EPL (Europhysics Letters)*, 101(2):20010, 2013.
40. Michael E. Cates and Julien Tailleur. Motility-induced phase separation. *Annual Review of Condensed Matter Physics*, 6(1):219–244, 2015.
41. Sara Dal Cengio, Demian Levis, and Ignacio Pagonabarraga. Fluctuation-dissipation relations in the absence of detailed balance: formalism and applications to active matter. *arXiv preprint arXiv:2007.07322*, 2020.
42. Debasish Chaudhuri and Abhishek Dhar. Active brownian particle in harmonic trap: exact computation of moments, and re-entrant transition. *arXiv preprint arXiv:2005.14234*, 2020.
43. Frank Cichos, Kristian Gustavsson, Bernhard Mehlig, and Giovanni Volpe. Machine learning for active matter. *Nature Machine Intelligence*, 2(2):94–103, 2020.

44. Jonathan Colen, Ming Han, Rui Zhang, Steven A Redford, Linnea M Lemma, Link Morgan, Paul V Ruijgrok, Raymond Adkins, Zev Bryant, Zvonimir Dogic, et al. Machine learning active-nematic hydrodynamics. *arXiv preprint arXiv:2006.13203*, 2020.
45. Leticia F Cugliandolo, Giuseppe Gonnella, and Isabella Petrelli. Effective temperature in active brownian particles. *Fluctuation and Noise Letters*, 18(02):1940008, 2019.
46. Lennart Dabelow, Stefano Bo, and Ralf Eichhorn. Irreversibility in active matter systems: Fluctuation theorem and mutual information. *Physical Review X*, 9(2):021009, 2019.
47. Lokrshi Prawar Dadhichi, Ananyo Maitra, and Sriram Ramaswamy. Origins and diagnostics of the nonequilibrium character of active systems. *Journal of Statistical Mechanics: Theory and Experiment*, 2018(12):123201, 2018.
48. Chengyu Dai, Isaac R Bruss, and Sharon C Glotzer. Phase separation and state oscillation of active inertial particles. *Soft Matter*, 16(11):2847–2853, 2020.
49. Sara Dal Cengio, Demian Levis, and Ignacio Pagonabarraga. Linear response theory and green-kubo relations for active matter. *Physical Review Letters*, 123(23):238003, 2019.
50. Olivier Dauchot and Vincent Démery. Dynamics of a self-propelled particle in a harmonic trap. *Physical review letters*, 122(6):068002, 2019.
51. Charlotte de Blois, Mathilde Reyssat, Sébastien Michelin, and Olivier Dauchot. Flow field around a confined active droplet. *Physical Review Fluids*, 4(5):054001, 2019.
52. Julien Deseigne, Olivier Dauchot, and Hugues Chaté. Collective motion of vibrated polar disks. *Physical review letters*, 105(9):098001, 2010.
53. Abhishek Dhar, Anupam Kundu, Satya N Majumdar, Sanjib Sabhapandit, and Grégory Schehr. Run-and-tumble particle in one-dimensional confining potentials: Steady-state, relaxation, and first-passage properties. *Physical Review E*, 99(3):032132, 2019.
54. R Di Leonardo, L Angelani, D Dell’Arciprete, Giancarlo Ruocco, V Iebba, S Schippa, MP Conte, F Mearini, F De Angelis, and E Di Fabrizio. Bacterial ratchet motors. *Proceedings of the National Academy of Sciences*, 107(21):9541–9545, 2010.
55. Pasquale Digregorio, Demian Levis, Antonio Suma, Leticia F Cugliandolo, Giuseppe Gonnella, and Ignacio Pagonabarraga. Full phase diagram of active brownian disks: From melting to motility-induced phase separation. *Physical review letters*, 121(9):098003, 2018.

56. L Dinis, P Martin, J Barral, J Prost, and JF Joanny. Fluctuation-response theorem for the active noisy oscillator of the hair-cell bundle. *Physical review letters*, 109(16):160602, 2012.
57. Jens Elgeti and Gerhard Gompper. Self-propelled rods near surfaces. *EPL (Europhysics Letters)*, 85(3):38002, 2009.
58. Jens Elgeti and Gerhard Gompper. Wall accumulation of self-propelled spheres. *EPL (Europhysics Letters)*, 101(4):48003, 2013.
59. Mihaela Enculescu and Holger Stark. Active colloidal suspensions exhibit polar order under gravity. *Physical review letters*, 107(5):058301, 2011.
60. Barath Ezhilan, Roberto Alonso-Matilla, and David Saintillan. On the distribution and swim pressure of run-and-tumble particles in confinement. *Journal of Fluid Mechanics*, 781, 2015.
61. Thomas FF Farage, Philip Krinninger, and Joseph M Brader. Effective interactions in active brownian suspensions. *Physical Review E*, 91(4):042310, 2015.
62. Richard P Feynman, Robert B Leighton, and Matthew Sands. The feynman lectures on physics; vol. i. *American Journal of Physics*, 33(9):750–752, 1965.
63. Yaouen Fily and M Cristina Marchetti. Athermal phase separation of self-propelled particles with no alignment. *Physical review letters*, 108(23):235702, 2012.
64. Andreas Fischer, Arky Chatterjee, and Thomas Speck. Aggregation and sedimentation of active brownian particles at constant affinity. *The Journal of chemical physics*, 150(6):064910, 2019.
65. É Fodor, M Guo, NS Gov, P Visco, DA Weitz, and F van Wijland. Activity-driven fluctuations in living cells. *EPL (Europhysics Letters)*, 110(4):48005, 2015.
66. Étienne Fodor, Wylie W Ahmed, Maria Almonacid, Matthias Bussonnier, Nir S Gov, M-H Verlhac, Timo Betz, Paolo Visco, and Frédéric van Wijland. Nonequilibrium dissipation in living oocytes. *EPL (Europhysics Letters)*, 116(3):30008, 2016.
67. Étienne Fodor, Vishwajeet Mehandia, Jordi Comelles, Raghavan Thiagarajan, Nir S Gov, Paolo Visco, Frédéric van Wijland, and Daniel Riveline. Spatial fluctuations at vertices of epithelial layers: quantification of regulation by rho pathway. *Biophysical journal*, 114(4):939–946, 2018.

68. Étienne Fodor, Cesare Nardini, Michael E. Cates, Julien Tailleur, Paolo Visco, and Frédéric van Wijland. How far from equilibrium is active matter? *Physical Review Letters*, 117:038103, Jul 2016.
69. Ronald F. Fox. Functional-calculus approach to stochastic differential equations. *Phys. Rev. A*, 33:467–476, 1986.
70. Ronald Forrest Fox. Uniform convergence to an effective fokker-planck equation for weakly colored noise. *Phys. Rev. A*, 34:4525–4527, 1986.
71. Giacomo Frangipane, Dario Dell’Arciprete, Serena Petracchini, Claudio Maggi, Filippo Saglimbeni, Silvio Bianchi, Gaszton Vizsnyiczai, Maria Lina Bernardini, and Roberto Di Leonardo. Dynamic density shaping of photokinetic e. coli. *Elife*, 7:e36608, 2018.
72. Peter Galajda, Juan Keymer, Paul Chaikin, and Robert Austin. A wall of funnels concentrates swimming bacteria. *Journal of bacteriology*, 189(23):8704–8707, 2007.
73. Chandrima Ganguly and Debasish Chaudhuri. Stochastic thermodynamics of active brownian particles. *Phys. Rev. E*, 88:032102, Sep 2013.
74. Crispin W Gardiner et al. *Handbook of stochastic methods*, volume 3. springer Berlin, 1985.
75. Pulak K Ghosh, Vyacheslav R Misko, Fabio Marchesoni, and Franco Nori. Self-propelled janus particles in a ratchet: Numerical simulations. *Physical review letters*, 110(26):268301, 2013.
76. Felix Ginot, Alexandre Solon, Yariv Kafri, Christophe Ybert, Julien Tailleur, and Cecile Cottin-Bizonne. Sedimentation of self-propelled janus colloids: polarization and pressure. *New Journal of Physics*, 20(11):115001, 2018.
77. Félix Ginot, Isaac Theurkauff, Demian Levis, Christophe Ybert, Lydéric Bocquet, Ludovic Berthier, and Cécile Cottin-Bizonne. Nonequilibrium equation of state in suspensions of active colloids. *Physical Review X*, 5(1):011004, 2015.
78. J Gladrow, N Fakhri, FC MacKintosh, CF Schmidt, and CP Broedersz. Broken detailed balance of filament dynamics in active networks. *Physical review letters*, 116(24):248301, 2016.
79. FS Gnesotto, Federica Mura, Jannes Gladrow, and Chase P Broedersz. Broken detailed balance and non-equilibrium dynamics in living systems: a review. *Reports on Progress in Physics*, 81(6):066601, 2018.

80. Giuseppe Gonnella, Davide Marenduzzo, Antonio Suma, and Adriano Tiribocchi. Motility-induced phase separation and coarsening in active matter. *Comptes Rendus Physique*, 16(3):316–331, 2015.
81. Yusuke Goto and Hajime Tanaka. Purely hydrodynamic ordering of rotating disks at a finite reynolds number. *Nature communications*, 6(1):1–10, 2015.
82. Tobias Grafke, Michael E Cates, and Eric Vanden-Eijnden. Spatiotemporal self-organization of fluctuating bacterial colonies. *Physical review letters*, 119(18):188003, 2017.
83. Omer Granek, Yongjoo Baek, Yariv Kafri, and Alexandre P Solon. Bodies in an interacting active fluid: far-field influence of a single body and interaction between two bodies. *Journal of Statistical Mechanics: Theory and Experiment*, 2020(6):063211, 2020.
84. Ming Guo, Allen J Ehrlicher, Mikkel H Jensen, Malte Renz, Jeffrey R Moore, Robert D Goldman, Jennifer Lippincott-Schwartz, Frederick C Mackintosh, and David A Weitz. Probing the stochastic, motor-driven properties of the cytoplasm using force spectrum microscopy. *Cell*, 158(4):822–832, 2014.
85. Ming Han, Jing Yan, Steve Granick, and Erik Luijten. Effective temperature concept evaluated in an active colloid mixture. *Proceedings of the National Academy of Sciences*, 114(29):7513–7518, 2017.
86. Peter Hänggi and Fabio Marchesoni. Artificial brownian motors: Controlling transport on the nanoscale. *Reviews of Modern Physics*, 81(1):387, 2009.
87. Takahiro Hatano and Shin-ichi Sasa. Steady-state thermodynamics of langevin systems. *Physical review letters*, 86(16):3463, 2001.
88. Marc Hennes, Katrin Wolff, and Holger Stark. Self-induced polar order of active brownian particles in a harmonic trap. *Physical review letters*, 112(23):238104, 2014.
89. Sophie Hermann and Matthias Schmidt. Active ideal sedimentation: exact two-dimensional steady states. *Soft Matter*, 14(9):1614–1621, 2018.
90. Jonathan R Howse, Richard AL Jones, Anthony J Ryan, Tim Gough, Reza Vafabakhsh, and Ramin Golestanian. Self-motile colloidal particles: from directed propulsion to random walk. *Physical review letters*, 99(4):048102, 2007.

91. Da-Quan Jiang, Donghua Jiang, and Min Qian. *Mathematical theory of nonequilibrium steady states: on the frontier of probability and dynamical systems*. Number 1833 in Lecture Notes in Mathematics. Springer Science & Business Media, 2004.
92. Frank Jülicher, Armand Ajdari, and Jacques Prost. Modeling molecular motors. *Reviews of Modern Physics*, 69(4):1269, 1997.
93. Peter Jung and Peter Hänggi. Dynamical systems: A unified colored-noise approximation. *Phys. Rev. A*, 35:4464–4466, 1987.
94. Juliane U Klamsler, Sebastian C Kapfer, and Werner Krauth. Thermodynamic phases in two-dimensional active matter. *Nature communications*, 9(1):1–8, 2018.
95. Juliane U Klamsler, Sebastian C Kapfer, and Werner Krauth. A kinetic-monte carlo perspective on active matter. *The Journal of chemical physics*, 150(14):144113, 2019.
96. MM Kłosek-Dygas, BJ Matkowsky, and Z Schuss. Colored noise in dynamical systems. *SIAM Journal on Applied Mathematics*, 48(2):425–441, 1988.
97. Gašper Kokot, Shibananda Das, Roland G Winkler, Gerhard Gompper, Igor S Aranson, and Alexey Snezhko. Active turbulence in a gas of self-assembled spinners. *Proceedings of the National Academy of Sciences*, 114(49):12870–12875, 2017.
98. Nn Koumakis, C Maggi, and R Di Leonardo. Directed transport of active particles over asymmetric energy barriers. *Soft matter*, 10(31):5695–5701, 2014.
99. Sudeesh Krishnamurthy, Subho Ghosh, Dipankar Chatterji, Rajesh Ganapathy, and AK Sood. A micrometre-sized heat engine operating between bacterial reservoirs. *Nature Physics*, 12(12):1134, 2016.
100. Jan-Timm Kuhr, Johannes Blaschke, Felix Rühle, and Holger Stark. Collective sedimentation of squirmers under gravity. *Soft matter*, 13(41):7548–7555, 2017.
101. Jorge Kurchan. Fluctuation theorem for stochastic dynamics. *Journal of Physics A: Mathematical and General*, 31(16):3719, 1998.
102. François A Lavergne, Hugo Wendehenne, Tobias Bäumler, and Clemens Bechinger. Group formation and cohesion of active particles with visual perception-dependent motility. *Science*, 364(6435):70–74, 2019.

103. Joel L Lebowitz and Herbert Spohn. A gallavotti–cohen-type symmetry in the large deviation functional for stochastic dynamics. *Journal of Statistical Physics*, 95(1-2):333–365, 1999.
104. Demian Levis and Ludovic Berthier. From single-particle to collective effective temperatures in an active fluid of self-propelled particles. *EPL (Europhysics Letters)*, 111(6):60006, 2015.
105. Demian Levis, Joan Codina, and Ignacio Pagonabarraga. Active brownian equation of state: metastability and phase coexistence. *Soft Matter*, 13(44):8113–8119, 2017.
106. Yan-Wei Li and Massimo Pica Ciamarra. Phase behavior of lennard-jones particles in two dimensions. *Physical Review E*, 102(6):062101, 2020.
107. Benno Liebchen, Michael E Cates, and Davide Marenduzzo. Pattern formation in chemically interacting active rotors with self-propulsion. *Soft Matter*, 12(35):7259–7264, 2016.
108. Davide Loi, Stefano Mossa, and Leticia F Cugliandolo. Effective temperature of active matter. *Physical Review E*, 77(5):051111, 2008.
109. Davide Loi, Stefano Mossa, and Leticia F Cugliandolo. Effective temperature of active complex matter. *Soft Matter*, 7(8):3726–3729, 2011.
110. Davide Loi, Stefano Mossa, and Leticia F Cugliandolo. Non-conservative forces and effective temperatures in active polymers. *Soft Matter*, 7(21):10193–10209, 2011.
111. Hartmut Löwen. Inertial effects of self-propelled particles: From active brownian to active langevin motion. *The Journal of Chemical Physics*, 152(4):040901, 2020.
112. Stefan Machlup and Lars Onsager. Fluctuations and irreversible process. ii. systems with kinetic energy. *Physical Review*, 91(6):1512, 1953.
113. Christian Maes. The fluctuation theorem as a gibbs property. *Journal of statistical physics*, 95(1):367–392, 1999.
114. Christian Maes. Fluctuating motion in an active environment. *arXiv preprint arXiv:2005.13462*, 2020.
115. Christian Maes. Frenesy: Time-symmetric dynamical activity in nonequilibria. *Physics Reports*, 850:1–33, 2020.
116. Christian Maes. Local detailed balance. *arXiv preprint arXiv:2011.09200*, 2020.

117. Claudio Maggi, Umberto Marini Bettolo Marconi, Nicoletta Gnan, and Roberto Di Leonardo. Multidimensional stationary probability distribution for interacting active particles. *Scientific reports*, 5:10742, 2015.
118. Claudio Maggi, Filippo Saglimbeni, Michele Dipalo, Francesco De Angelis, and Roberto Di Leonardo. Micromotors with asymmetric shape that efficiently convert light into work by thermocapillary effects. *Nature communications*, 6:7855, 2015.
119. Marcelo O Magnasco. Forced thermal ratchets. *Physical Review Letters*, 71(10):1477, 1993.
120. Saeed Mahdisoltani, Riccardo Ben Ali Zinati, Charlie Duclut, Andrea Gambassi, and Ramin Golestanian. Controlled dynamics and number fluctuations with two strategies for quorum sensing. *arXiv preprint arXiv:1911.08115*, 2019.
121. Kanaya Malakar, Arghya Das, Anupam Kundu, K Vijay Kumar, and Abhishek Dhar. Steady state of an active brownian particle in a two-dimensional harmonic trap. *Physical Review E*, 101(2):022610, 2020.
122. Emil Mallmin, Richard A Blythe, and Martin R Evans. Exact spectral solution of two interacting run-and-tumble particles on a ring lattice. *Journal of Statistical Mechanics: Theory and Experiment*, 2019(1):013204, 2019.
123. A Manacorda and A Puglisi. Lattice model to derive the fluctuating hydrodynamics of active particles with inertia. *Physical review letters*, 119(20):208003, 2017.
124. Dibyendu Mandal, Katherine Klymko, and Michael R DeWeese. Entropy production and fluctuation theorems for active matter. *Physical review letters*, 119(25):258001, 2017.
125. Suvendu Mandal, Benno Liebchen, and Hartmut Löwen. Motility-induced temperature difference in coexisting phases. *Physical Review Letters*, 123(22):228001, 2019.
126. MC Marchetti, JF Joanny, S Ramaswamy, TB Liverpool, J Prost, Madan Rao, and R Aditi Simha. Hydrodynamics of soft active matter. *Reviews of Modern Physics*, 85(3):1143, 2013.
127. Umberto Marini Bettolo Marconi and Claudio Maggi. Towards a statistical mechanical theory of active fluids. *Soft matter*, 11(45):8768–8781, 2015.
128. David Martin. Aoup in the presence of brownian noise: a perturbative approach. *arXiv preprint arXiv:2009.13476*, 2020.

129. David Martin, Jérémy O’Byrne, Michael E Cates, Étienne Fodor, Cesare Nardini, Julien Tailleur, and Frédéric van Wijland. Statistical mechanics of active ornstein uhlenbeck particles. *arXiv preprint arXiv:2008.12972*, 2020.
130. AJ McKane, HC Luckock, and AJ Bray. Path integrals and non-markov processes. i. general formalism. *Physical Review A*, 41(2):644, 1990.
131. Daisuke Mizuno, Catherine Tardin, Christoph F Schmidt, and Frederik C MacKintosh. Nonequilibrium mechanics of active cytoskeletal networks. *Science*, 315(5810):370–373, 2007.
132. Thierry Mora, Aleksandra M Walczak, Lorenzo Del Castello, Francesco Ginelli, Stefania Melillo, Leonardo Parisi, Massimiliano Viale, Andrea Cavagna, and Irene Giardina. Local equilibrium in bird flocks. *Nature physics*, 12(12):1153, 2016.
133. Konstantin I Morozov and Len M Pismen. Motor-driven effective temperature and viscoelastic response of active matter. *Physical Review E*, 81(6):061922, 2010.
134. Cesare Nardini, Étienne Fodor, Elsen Tjhung, Frédéric van Wijland, Julien Tailleur, and Michael E. Cates. Entropy production in field theories without time-reversal symmetry: Quantifying the non-equilibrium character of active matter. *Phys. Rev. X*, 7:021007, Apr 2017.
135. RW Nash, R Adhikari, J Tailleur, and ME Cates. Run-and-tumble particles with hydrodynamics: Sedimentation, trapping, and upstream swimming. *Physical review letters*, 104(25):258101, 2010.
136. Takahiro Nemoto, Étienne Fodor, Michael E Cates, Robert L Jack, and Julien Tailleur. Optimizing active work: Dynamical phase transitions, collective motion, and jamming. *Physical Review E*, 99(2):022605, 2019.
137. Nguyen HP Nguyen, Daphne Klotsa, Michael Engel, and Sharon C Glotzer. Emergent collective phenomena in a mixture of hard shapes through active rotation. *Physical review letters*, 112(7):075701, 2014.
138. Nikolai Nikola, Alexandre P Solon, Yariv Kafri, Mehran Kardar, Julien Tailleur, and Raphaël Voituriez. Active particles with soft and curved walls: Equation of state, ratchets, and instabilities. *Physical review letters*, 117(9):098001, 2016.
139. Daiki Nishiguchi and Masaki Sano. Mesoscopic turbulence and local order in janus particles self-propelling under an ac electric field. *Physical Review E*, 92(5):052309, 2015.

140. Lars Onsager and Stefan Machlup. Fluctuations and irreversible processes. *Physical Review*, 91(6):1505, 1953.
141. Jérémy O’Byrne and Julien Tailleur. Lamellar to micellar phases and beyond: When tactic active systems admit free energy functionals. *Physical Review Letters*, 125(20):208003, 2020.
142. Jérémie Palacci, Cécile Cottin-Bizonne, Christophe Ybert, and Lydéric Bocquet. Sedimentation and effective temperature of active colloidal suspensions. *Physical Review Letters*, 105(8):088304, 2010.
143. Jeremie Palacci, Stefano Sacanna, Asher Preska Steinberg, David J Pine, and Paul M Chaikin. Living crystals of light-activated colloidal surfers. *Science*, 339(6122):936–940, 2013.
144. Siddharth Paliwal, Vasileios Prymidis, Laura Filion, and Marjolein Dijkstra. Non-equilibrium surface tension of the vapour-liquid interface of active lennard-jones particles. *The Journal of chemical physics*, 147(8):084902, 2017.
145. Siddharth Paliwal, Jeroen Rodenburg, René van Roij, and Marjolein Dijkstra. Chemical potential in active systems: predicting phase equilibrium from bulk equations of state? *New Journal of Physics*, 20(1):015003, 2018.
146. Juan MR Parrondo and Pep Español. Criticism of feynman’s analysis of the ratchet as an engine. *American Journal of Physics*, 64(9):1125–1130, 1996.
147. Patrick Pietzonka and Udo Seifert. Entropy production of active particles and for particles in active baths. *Journal of Physics A: Mathematical and Theoretical*, 51(1):01LT01, 2017.
148. A Pototsky and H Stark. Active brownian particles in two-dimensional traps. *EPL (Europhysics Letters)*, 98(5):50004, 2012.
149. Andrey Pototsky, Aljoscha M Hahn, and Holger Stark. Rectification of self-propelled particles by symmetric barriers. *Physical Review E*, 87(4):042124, 2013.
150. Mathieu Poujade, Erwan Grasland-Mongrain, A Hertzog, J Jouanneau, Philippe Chavier, Benoît Ladoux, Axel Buguin, and Pascal Silberzan. Collective migration of an epithelial monolayer in response to a model wound. *Proceedings of the National Academy of Sciences*, 104(41):15988–15993, 2007.
151. Jacques Prost, J-F Joanny, and Juan MR Parrondo. Generalized fluctuation-dissipation theorem for steady-state systems. *Physical review letters*, 103(9):090601, 2009.

152. Gabriel S Redner, Aparna Baskaran, and Michael F Hagan. Reentrant phase behavior in active colloids with attraction. *Physical Review E*, 88(1):012305, 2013.
153. Gabriel S Redner, Michael F Hagan, and Aparna Baskaran. Structure and dynamics of a phase-separating active colloidal fluid. *Physical review letters*, 110(5):055701, 2013.
154. Gabriel S Redner, Caleb G Wagner, Aparna Baskaran, and Michael F Hagan. Classical nucleation theory description of active colloid assembly. *Physical review letters*, 117(14):148002, 2016.
155. Markus Rein and Thomas Speck. Applicability of effective pair potentials for active brownian particles. *The European Physical Journal E*, 39(9):84, 2016.
156. David Richard, Hartmut Löwen, and Thomas Speck. Nucleation pathway and kinetics of phase-separating active brownian particles. *Soft Matter*, 12(24):5257–5264, 2016.
157. Hannes Risken. Fokker-planck equation. In *The Fokker-Planck Equation*. Springer, 1996.
158. Sunghan Ro, Yariv Kafri, Mehran Kardar, and Julien Tailleur. Disorder-induced long-ranged correlations in scalar active matter. *arXiv preprint arXiv:2007.12670*, 2020.
159. Damien Robert, Thi-Hanh Nguyen, François Gallet, and Claire Wilhelm. In vivo determination of fluctuating forces during endosome trafficking using a combination of active and passive microrheology. *PloS one*, 5(4):e10046, 2010.
160. Édgar Roldán, Jérémie Barral, Pascal Martin, Juan MR Parrondo, and Frank Jülicher. Arrow of time in active fluctuations. *arXiv preprint arXiv:1803.04743*, 2018.
161. Pawel Romanczuk, Markus Bär, Werner Ebeling, Benjamin Lindner, and Lutz Schimansky-Geier. Active brownian particles. *The European Physical Journal Special Topics*, 202(1):1–162, 2012.
162. Syeda Sabrina, Mykola Tasinkevych, Suzanne Ahmed, Allan M Brooks, Monica Olvera de la Cruz, Thomas E Mallouk, and Kyle JM Bishop. Shape-directed microspinners powered by ultrasound. *ACS nano*, 12(3):2939–2947, 2018.
163. Suropriya Saha, Ramin Golestanian, and Sriram Ramaswamy. Clusters, asters, and collective oscillations in chemotactic colloids. *Physical Review E*, 89(6):062316, 2014.

164. Jonathan Saragosti, Vincent Calvez, Nikolaos Bournaveas, Benoit Perthame, Axel Buguin, and Pascal Silberzan. Directional persistence of chemotactic bacteria in a traveling concentration wave. *Proceedings of the National Academy of Sciences*, 108(39):16235–16240, 2011.
165. Paolo Sartori, Enrico Chiarello, Gaurav Jayaswal, Matteo Pierno, Giampaolo Mistura, Paola Brun, Adriano Tiribocchi, and Enzo Orlandini. Wall accumulation of bacteria with different motility patterns. *Physical Review E*, 97(2):022610, 2018.
166. Mark J Schnitzer. Theory of continuum random walks and application to chemotaxis. *Physical Review E*, 48(4):2553, 1993.
167. Udo Seifert. Entropy production along a stochastic trajectory and an integral fluctuation theorem. *Physical review letters*, 95(4):040602, 2005.
168. Ken Sekimoto. Kinetic characterization of heat bath and the energetics of thermal ratchet models. *Journal of the physical society of Japan*, 66(5):1234–1237, 1997.
169. Suraj Shankar and M Cristina Marchetti. Hidden entropy production and work fluctuations in an ideal active gas. *Physical Review E*, 98(2):020604, 2018.
170. Xia-qing Shi, Giordano Fausti, Hugues Chaté, Cesare Nardini, and Alexandre Solon. Self-organized critical coexistence phase in repulsive active particles. *Physical Review Letters*, 125(16):168001, 2020.
171. Marian Smoluchowski. Experimentell nachweisbare, der üblichen thermodynamik widersprechende molekularphänomene. *Pisma Mariana Smoluchowskiego*, 2(1):226–251, 1927.
172. Andrey Sokolov, Mario M Apodaca, Bartosz A Grzybowski, and Igor S Aranson. Swimming bacteria power microscopic gears. *Proceedings of the National Academy of Sciences*, 107(3):969–974, 2010.
173. Alexandre P Solon, ME Cates, and Julien Tailleur. Active brownian particles and run-and-tumble particles: A comparative study. *The European Physical Journal Special Topics*, 224(7):1231–1262, 2015.
174. Alexandre P Solon, Hugues Chaté, and Julien Tailleur. From phase to microphase separation in flocking models: The essential role of nonequilibrium fluctuations. *Physical review letters*, 114(6):068101, 2015.

175. Alexandre P Solon, Y Fily, Aparna Baskaran, Mickael E Cates, Y Kafri, M Kardar, and J Tailleur. Pressure is not a state function for generic active fluids. *Nature Physics*, 11(8):673, 2015.
176. Alexandre P Solon, Joakim Stenhammar, Michael E Cates, Yariv Kafri, and Julien Tailleur. Generalized thermodynamics of motility-induced phase separation: phase equilibria, laplace pressure, and change of ensembles. *New Journal of Physics*, 20(7):075001, 2018.
177. Alexandre P Solon, Joakim Stenhammar, Michael E Cates, Yariv Kafri, and Julien Tailleur. Generalized thermodynamics of phase equilibria in scalar active matter. *Physical Review E*, 97(2):020602, 2018.
178. Vishal Soni, Ephraim S Bililign, Sofia Magkiriadou, Stefano Sacanna, Denis Bartolo, Michael J Shelley, and William TM Irvine. The odd free surface flows of a colloidal chiral fluid. *Nature Physics*, 15(11):1188–1194, 2019.
179. Rodrigo Soto and Ramin Golestanian. Run-and-tumble dynamics in a crowded environment: Persistent exclusion process for swimmers. *Physical Review E*, 89(1):012706, 2014.
180. Thomas Speck, Julian Bialké, Andreas M Menzel, and Hartmut Löwen. Effective cahn-hilliard equation for the phase separation of active brownian particles. *Physical Review Letters*, 112(21):218304, 2014.
181. Joakim Stenhammar, Raphael Wittkowski, Davide Marenduzzo, and Michael E Cates. Light-induced self-assembly of active rectification devices. *Science advances*, 2(4):e1501850, 2016.
182. Antonio Suma, Giuseppe Gonnella, Gianluca Laghezza, Antonio Lamura, Alessandro Mossa, and Leticia F Cugliandolo. Dynamics of a homogeneous active dumbbell system. *Physical Review E*, 90(5):052130, 2014.
183. Grzegorz Szamel. Self-propelled particle in an external potential: Existence of an effective temperature. *Physical Review E*, 90(1):012111, 2014.
184. Grzegorz Szamel. Stochastic thermodynamics for self-propelled particles. *Physical Review E*, 100(5):050603, 2019.
185. J Tailleur and ME Cates. Statistical mechanics of interacting run-and-tumble bacteria. *Physical review letters*, 100(21):218103, 2008.

186. J Tailleur and ME Cates. Sedimentation, trapping, and rectification of dilute bacteria. *EPL (Europhysics Letters)*, 86(6):60002, 2009.
187. Julien Tailleur, Jorge Kurchan, and Vivien Lecomte. Mapping out-of-equilibrium into equilibrium in one-dimensional transport models. *Journal of Physics A: Mathematical and Theoretical*, 41(50):505001, 2008.
188. Sho C Takatori and John F Brady. Towards a thermodynamics of active matter. *Physical Review E*, 91(3):032117, 2015.
189. Sho C Takatori, Raf De Dier, Jan Vermant, and John F Brady. Acoustic trapping of active matter. *Nature communications*, 7(1):1–7, 2016.
190. Sorin Tanase-Nicola and Jorge Kurchan. Statistical-mechanical formulation of lyapunov exponents. *Journal of Physics A: Mathematical and General*, 36(41):10299, 2003.
191. AG Thompson, J Tailleur, ME Cates, and RA Blythe. Lattice models of nonequilibrium bacterial dynamics. *Journal of Statistical Mechanics: Theory and Experiment*, 2011(02):P02029, 2011.
192. Shashi Thutupalli, Delphine Geyer, Rajesh Singh, Ronjoy Adhikari, and Howard A Stone. Flow-induced phase separation of active particles is controlled by boundary conditions. *Proceedings of the National Academy of Sciences*, 115(21):5403–5408, 2018.
193. Elsen Tjhung, Cesare Nardini, and Michael E Cates. Cluster phases and bubbly phase separation in active fluids: reversal of the ostwald process. *Physical Review X*, 8(3):031080, 2018.
194. John Toner and Yuhai Tu. Long-range order in a two-dimensional dynamical xy model: how birds fly together. *Physical Review Letters*, 75(23):4326, 1995.
195. Francesco Turci and Nigel B Wilding. Phase separation and multibody effects in three-dimensional active brownian particles. *Physical Review Letters*, 126(3):038002, 2021.
196. Christian Van den Broeck and Peter Hänggi. Activation rates for nonlinear stochastic flows driven by non-gaussian noise. *Physical Review A*, 30(5):2730, 1984.
197. Marjolein N van der Linden, Lachlan C Alexander, Dirk GAL Aarts, and Olivier Dauchot. Interrupted motility induced phase separation in aligning active colloids. *Physical review letters*, 123(9):098001, 2019.

198. NG Van Kampen. Relative stability in nonuniform temperature. *IBM Journal of Research and Development*, 32(1):107–111, 1988.
199. Nicolaas Godfried Van Kampen. *Stochastic processes in physics and chemistry*, volume 1. Elsevier, 1992.
200. Benjamin C van Zuiden, Jayson Paulose, William TM Irvine, Denis Bartolo, and Vincenzo Vitelli. Spatiotemporal order and emergent edge currents in active spinner materials. *Proceedings of the national academy of sciences*, 113(46):12919–12924, 2016.
201. Tamás Vicsek, András Czirók, Eshel Ben-Jacob, Inon Cohen, and Ofer Shochet. Novel type of phase transition in a system of self-driven particles. *Physical review letters*, 75(6):1226, 1995.
202. Tamás Vicsek and Anna Zafeiris. Collective motion. *Physics Reports*, 517(3):71–140, 2012.
203. Caleb G Wagner, Michael F Hagan, and Aparna Baskaran. Steady-state distributions of ideal active brownian particles under confinement and forcing. *Journal of Statistical Mechanics: Theory and Experiment*, 2017(4):043203, 2017.
204. Shenshen Wang and Peter G. Wolynes. Communication: Effective temperature and glassy dynamics of active matter. *The Journal of Chemical Physics*, 135(5):051101, 2011.
205. Claire Wilhelm. Out-of-equilibrium microrheology inside living cells. *Physical review letters*, 101(2):028101, 2008.
206. Edward Witten et al. Supersymmetry and morse theory. *Journal of differential geometry*, 17(4):661–692, 1982.
207. Raphael Wittkowski, Adriano Tiribocchi, Joakim Stenhammar, Rosalind J Allen, Davide Marenduzzo, and Michael E Cates. Scalar φ^4 field theory for active-particle phase separation. *Nature communications*, 5(1):1–9, 2014.
208. René Wittmann, Claudio Maggi, Abhinav Sharma, Alberto Scacchi, Joseph M Brader, and U Marini Bettolo Marconi. Effective equilibrium states in the colored-noise model for active matter i. pairwise forces in the fox and unified colored noise approximations. *Journal of Statistical Mechanics: Theory and Experiment*, 2017(11):113207, 2017.
209. René Wittmann, U Marini Bettolo Marconi, Claudio Maggi, and Joseph M Brader. Effective equilibrium states in the colored-noise model for active matter ii. a unified framework

- for phase equilibria, structure and mechanical properties. *Journal of Statistical Mechanics: Theory and Experiment*, 2017(11):113208, 2017.
210. E. Woillez, Y. Zhao, Y. Kafri, V. Lecomte, and J. Tailleur. Activated escape of a self-propelled particle from a metastable state. *Phys. Rev. Lett.*, 122:258001, Jun 2019.
211. Eric Woillez, Yariv Kafri, and Vivien Lecomte. Nonlocal stationary probability distributions and escape rates for an active ornstein–uhlenbeck particle. *Journal of Statistical Mechanics: Theory and Experiment*, 2020(6):063204, 2020.
212. Katrin Wolff, Aljoscha M Hahn, and Holger Stark. Sedimentation and polar order of active bottom-heavy particles. *The European Physical Journal E*, 36(4):43, 2013.
213. Jing Yan, Ming Han, Jie Zhang, Cong Xu, Erik Luijten, and Steve Granick. Reconfiguring active particles by electrostatic imbalance. *Nature materials*, 15(10):1095–1099, 2016.
214. Xingbo Yang, M Lisa Manning, and M Cristina Marchetti. Aggregation and segregation of confined active particles. *Soft matter*, 10(34):6477–6484, 2014.
215. Ehud Yariv and Ory Schnitzer. Ratcheting of brownian swimmers in periodically corrugated channels: A reduced fokker-planck approach. *Physical Review E*, 90(3):032115, 2014.
216. Kyongmin Yeo, Enkeleida Lushi, and Petia M Vlahovska. Collective dynamics in a binary mixture of hydrodynamically coupled microrotors. *Physical review letters*, 114(18):188301, 2015.